Interaction of the human prostacyclin receptor with the PDZ adapter protein PDZK1: role in endothelial cell migration and angiogenesis

Elizebeth C. Turner*, Eamon P. Mulvaney*, Helen M. Reid, and B. Therese Kinsella
School of Biomolecular and Biomedical Sciences, Conway Institute of Biomolecular and Biomedical Research, University College Dublin, Belfield, Dublin 4, Ireland

ABSTRACT **Prostacyclin is increasingly implicated in re-endothelialization and angiogenesis but through largely unknown mechanisms. Herein the high-density lipoprotein (HDL) scavenger receptor class B, type 1 (SR-B1) adapter protein PDZ domain-containing protein 1 (PDZK1) was identified as an interactant of the human prostacyclin receptor (hIP) involving a Class I PDZ ligand at its carboxyl terminus and PDZ domains 1, 3, and 4 of PDZK1. Although the interaction is constitutive, it may be dynamically regulated following cicaprost activation of the hIP through a mechanism involving cAMP-dependent protein kinase (PK)A-phosphorylation of PDZK1 at Ser-505. Although PDZK1 did not increase overall levels of the hIP, it increased its functional expression at the cell surface, enhancing ligand binding and cicaprost-induced cAMP generation. Consistent with its role in re-endothelialization and angiogenesis, cicaprost activation of the hIP increased endothelial cell migration and tube formation/in vitro angiogenesis, effects completely abrogated by the specific IP antagonist RO1138452. Furthermore, similar to HDL/SR-B1, small interfering RNA (siRNA)-targeted disruption of PDZK1 abolished cicaprost-mediated endothelial responses but did not affect VEGF responses. Considering the essential role played by prostacyclin throughout the cardiovascular system, identification of PDZK1 as a functional interactant of the hIP sheds significant mechanistic insights into the protective roles of these key players, and potentially HDL/SR-B1, within the vascular endothelium.**

Monitoring Editor
Carole A. Parent
National Institutes of Health

Received: Apr 28, 2011
Revised: May 24, 2011
Accepted: May 27, 2011

INTRODUCTION

Eukaryotic proteins are modular by nature. The frequently encountered postsynaptic density-95, disks large, zonula occludens-1 (PDZ) domain mediates protein:protein interactions by binding to the PDZ ligand located most typically, but not exclusively, at the extreme C termini of target proteins (Jemth and Gianni, 2007; Tonikian *et al.*, 2008; Lee and Zheng, 2010). Through the formation of multiprotein complexes, PDZ interactions can participate in the coordination of key intra- and intercellular signaling systems, including intracellular routing or localization of proteins, cell polarity, as well as in the regulation of cell:cell interactions (Jemth and Gianni, 2007; Tonikian *et al.*, 2008; Lee and Zheng, 2010). Structurally, the PDZ domain is composed of compact globular modules containing six anti-parallel β-strands (βA–βF) and two α-helices (αA and αB) with a highly conserved GLGF motif within its hydrophobic binding pocket that is responsible for the sequence-specific recognition of the PDZ ligand within the target protein(s). Depending on the nature of the three residues at their extreme C termini, the PDZ ligand of the target protein itself may belong to one of three classes, namely class I (Ser/Thr-X-Φ-COOH), class II (Φ-X-Φ-COOH), or class III (Asp/Glu-X-Φ-COOH), where Φ represents a hydrophobic amino acid and X can be any residue (Jemth and Gianni, 2007; Tonikian *et al.*, 2008; Lee and Zheng, 2010).

This article was published online ahead of print in MBoC in Press (http://www.molbiolcell.org/cgi/doi/10.1091/mbc.E11-04-0374) on June 8, 2011.

*These authors contributed equally to this work.

Address correspondence to: B. Therese Kinsella (Therese.Kinsella@UCD.IE).

Abbreviations used: DDO, double drop-out; FTI, Farnesyl transferase inhibitor; HA, hemagglutinin; HDL, high-density lipoprotein; hIP, human prostacyclin receptor; HUVEC, human umbilical vein endothelial cell; IP, prostacyclin receptor; PDZ, Postsynaptic density-95, Disks large, Zonula occludens-1; PDZK1, PDZ domain-containing protein 1; PKA, cAMP-dependent protein kinase A; PPAR, peroxisome proliferator-activated receptor; QDO, quadruple drop-out; RBD, Rab11 binding domain; si, small interfering; TP, thromboxane receptor; Y2H, yeast-two-hybrid.

The intracellular scaffold or adapter protein PDZ domain-containing protein 1 (PDZK1) is a member of the Na^+, H^+ exchanger regulatory family (NHERF) and is predominantly expressed in the brush border of the kidney and small intestine, in epithelial and endothelial cells, in macrophages, and in the liver (Kocher *et al.*, 1998; Lamprecht and Seidler, 2006; Kocher and Krieger, 2009). PDZK1 contains four PDZ domains, facilitating its binding to highly specific interacting partners, including various ion transporters (e.g., the cystic fibrosis transmembrane conductance regulator [CFTR] and apical organic cation transporters OCTN1 and OCTN2), inducible nitric oxide synthase, and certain members of the G-protein coupled receptor (GPCR) superfamily (Kato *et al.*, 2005; Navarro-Lerida *et al.*, 2007; Hu *et al.*, 2009). Most notably, through its interaction with the high-density lipoprotein (HDL) high-affinity scavenger receptor class B, type 1 (SR-B1), PDZK1 is essential for both reverse cholesterol transport and for HDL-mediated vascular re-endothelialization (Zhu *et al.*, 2008; Kocher and Krieger, 2009). More specifically, by binding to its C-terminal PDZ ligand, PDZK1 plays an essential role in maintaining hepatic SR-BI levels, thereby controlling HDL cholesterol levels, and is now also known to play a key role in HDL/SR-BI–dependent regulation of endothelial cell migration, promoting re-endothelialization and protecting against the development of atherosclerosis (Kocher *et al.*, 2003; Zhu *et al.*, 2008; Fenske *et al.*, 2009).

The prostanoid prostacyclin, or prostaglandin I_2, plays a central role in hemostasis, acting as a potent inhibitor of platelet aggregation and as an endothelium-derived vasodilator (Gryglewski, 2008; Kawabe *et al.*, 2010a). It exerts an important cytoprotective role within the myocardium (Ribeiro *et al.*, 1981) and, within the wider vasculature, promotes angiogenesis and limits restenosis, promoting re-endothelialiazation/vascular repair in response to injury (Kawabe *et al.*, 2010a). The importance of prostacyclin for hemostasis and cardiovascular integrity has been highlighted by the finding that certain COXIBs, selective inhibitors of cyclooxygenase 2, disproportionately depress prostacyclin generation, leaving subjects at increased risk of thrombotic stroke and myocardial infarction (Fitzgerald, 2004). Moreover, prostacyclin receptor ($IP^{-/-}$) null mice display enhanced tendency toward thrombosis, intima hyperplasia, atherosclerosis, and restenosis (Murata *et al.*, 1997; Yuhki *et al.*, 2011). More recently, in an experimental model of endothelial damage, it was established that endothelial progenitor cells (EPCs) from $IP^{-/-}$ null mice fail to promote re-endothelialization and vessel repair (Kawabe *et al.*, 2010b). Hence, somewhat similar to the HDL/SR-B1–mediated pathway, the prostacyclin receptor (IP) plays a central protective role in promoting re-endothelialization, limiting neointima hyperplasia and vascular remodeling in response to vessel wall injury that frequently accompanies atherosclerosis or surgical procedures, such as angioplasty or carotid endarterectomy, for example (Qu *et al.*, 2009; Kawabe *et al.*, 2010b). Somewhat consistent with this, several single-nucleotide polymorphisms have been identified within the IP gene that predispose individuals to cardiovascular (CV) disease, including enhanced risk of deep vein thrombosis and intimal hyperplasia (Arehart *et al.*, 2008; Patrignani *et al.*, 2008).

Although, as stated, prostacyclin mainly signals through the IP, a member of the GPCR superfamily (Gryglewski, 2008; Kawabe *et al.*, 2010a), it can also modulate the peroxisome proliferator-activated receptor (PPAR)δ signaling pathway(s), also with important clinical implications for angiogenesis (Pola *et al.*, 2004; Biscetti *et al.*, 2008, 2009; Biscetti and Pola, 2008; He *et al.*, 2008). The IP is primarily coupled to Gs/adenylyl cylase activation but may regulate other effectors in a cell- and/or species-specific manner (Lawler *et al.*, 2001b; Miggin *et al.*, 2002). The IP is somewhat unique among GPCRs in that it undergoes both isoprenylation and palmitoylation within its carboxyl-terminal tail (C-tail) domain, modifications that are critical for its signaling and function and intracellular trafficking (Hayes *et al.*, 1999; Lawler *et al.*, 2001a; Miggin *et al.*, 2002, 2003; O'Meara and Kinsella, 2004a, 2004b, 2005; Reid *et al.*, 2010). More specifically, the human IP (hIP) undergoes farnesylation at Cys^{383} within its carboxy-terminal conserved -$C^{383}SLC^{386}$, or 'CaaX', motif (Hayes *et al.*, 1999; Miggin *et al.*, 2002) and palmitoylation at Cys^{308}, Cys^{309}, and Cys^{311}, residues adjacent to a recently identified Rab11 binding domain (RBD) within the proximal C-tail of the hIP (Miggin *et al.*, 2003; Reid *et al.*, 2010).

Although, as stated, recent emerging data further highlight a central role for prostacyclin and the IP as a critical protective agent within the vascular endothelium, the underlying mechanisms whereby they do so remain to be defined. Herein we report the identification of a novel specific interaction between the hIP and the intracellular SR-B1 adapter protein PDZK1. The aim of this study was to characterize this novel protein:protein interaction and to explore its impact on hIP function, not least within vascular endothelial cells. Data presented herein identify a novel mechanism of agonist-regulated interaction of PDZK1 with the hIP involving direct cAMP-dependent PKA phosphorylation of PDZK1 in response to agonist-activation of the hIP itself. Moreover, in the context of re-endothelialization, it was established that, similar to SR-B1, the interaction of the hIP with PDZK1 is functionally critical for prostacyclin-mediated endothelial cell migration and angiogenesis in recognized in vitro models. Bearing in mind the critical roles of the hIP, PDZK1, and, indeed, SR-B1 within the vascular endothelium (Kocher and Krieger, 2009; Kawabe *et al.*, 2010a), the discovery of the interaction between the hIP and PDZK1 is likely to shed significant new insights into the mechanistic processes involved in endothelial integrity and in protection against CV disease.

RESULTS

Identification of PDZK1 as an interactant of the hIP in yeast and mammalian cells

We recently carried out a yeast-two-hybrid (Y2H) screen of a human kidney cDNA library to identify proteins that specifically interact with the carboxyl (C)-terminal tail domain of the hIP ($hIP^{299–386}$; Figure 1A). Through those studies, Rab11a was identified as a direct binding partner of the hIP through an interaction dependent on a 14-residue RBD located within its proximal C-tail domain, comprising Val^{299}–Val^{307} adjacent to the palmitoylated residues at Cys^{308}–Cys^{311} (Wikstrom *et al.*, 2008; Reid *et al.*, 2010). Herein we report the identification of the intracellular adapter protein PDZK1 as a direct interactant of the hIP. Using the $hIP^{299–386}$ as the initial bait protein, Y2H screening identified several independent clones that encode amino acids 1–154 of PDZK1 ($PDZK1^{1–154}$), encompassing its entire PDZ domain 1 (PDZ^{D1}) and part of its PDZ^{D2} (Hu *et al.*, 2009; LaLonde and Bretscher, 2009).

To initially investigate specificity, the interaction of $PDZK1^{1–154}$ was examined through extended Y2H mating-type studies with various subfragments of the C-tail domain derived from either the wild-type ($hIP^{299–386,WT}$) or isoprenylation-defective ($hIP^{299–386,SSLC}$) forms of the hIP (Wikstrom *et al.*, 2008; Reid *et al.*, 2010). As controls for those studies, the interaction of $PDZK1^{1–154}$ with the C-tail domains of the TPα ($TP\alpha^{312–343}$) and TPβ ($TP\beta^{312–407}$) isoforms of the human thromboxane (TX) A_2 receptor was examined, while comparison of the interaction of the hIP-derived subfragments with $PDZK1^{1–154}$ relative to that of Rab11a served as additional reference controls (Figure 1B). While all of the bait and prey yeast strains mated successfully to form diploids (Figure 1B, DDO), $PDZK1^{1–154}$ only interacted with subfragments containing the C-terminal residues of the

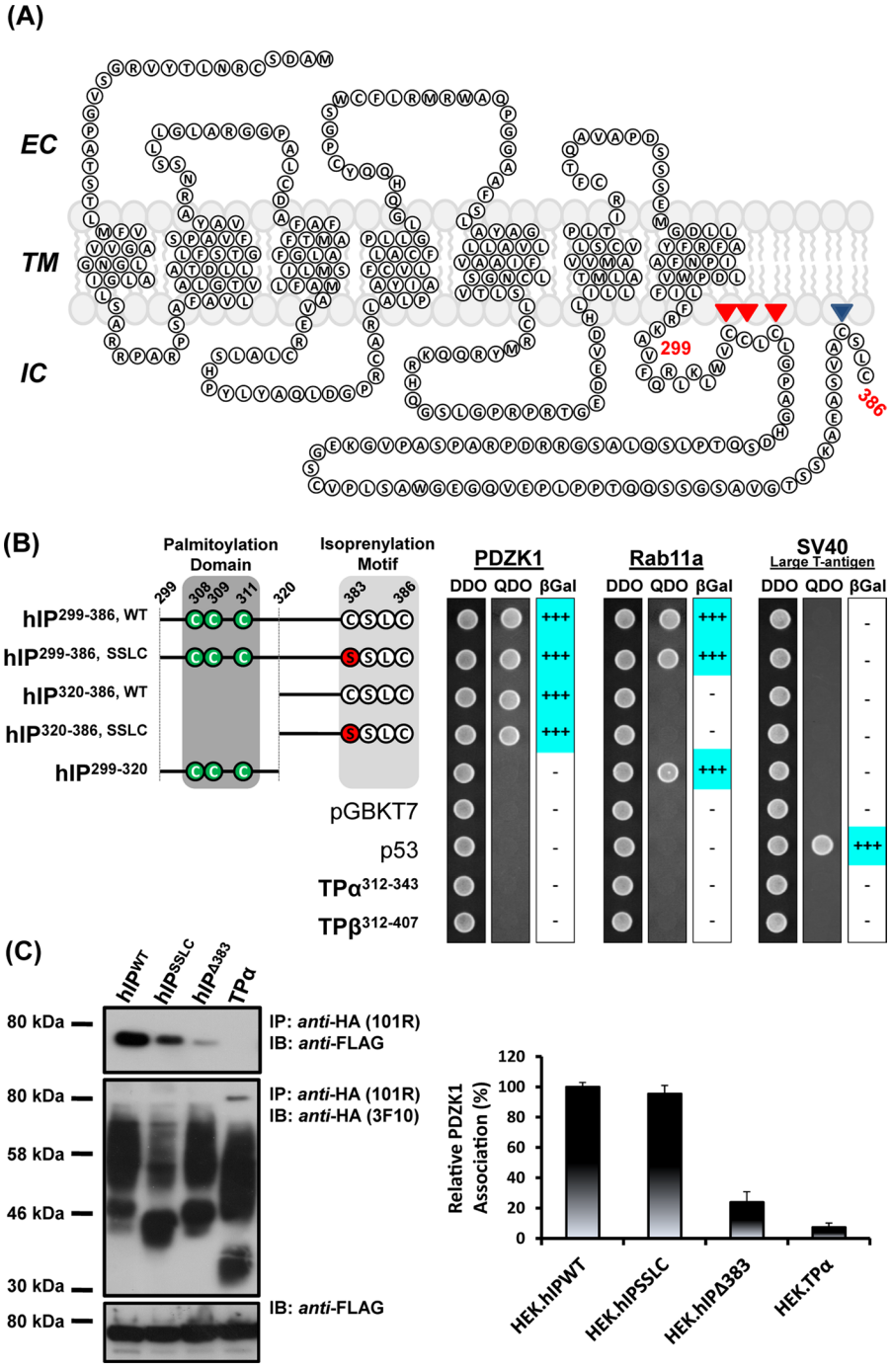

FIGURE 1. Interaction of PDZK1 with the human prostacyclin receptor. (A) Schematic of the hIP. The hIP undergoes palmitoylation at Cys^{308}, Cys^{309}, and Cys^{311} and isoprenylation/farnesylation at Cys^{383}, which, together, are proposed to introduce fourth (IC_4) and fifth (IC_5) intracellular loops within the C-tail domain of the hIP. (B) *S.c* Y187 (pACT2:PDZK1) or, as controls, *S.c* Y187 (pACT2:Rab11a) and *S.c* Y187 (pTD1-1), encoding SV-40 large T-antigen, prey strains were mated with *S.c* AH109 bait strains transformed with recombinant pGBKT7 encoding the listed hIP subfragments and, as controls, pGBKT7.TPα, pGBKT7.TPβ and p53 or with the vector pGBKT7 alone. Diploids were selected on DDO medium, whereas interactants were selected on QDO medium and by their ability to express β-galactosidase (β-Gal). Data: n ≥ 3. (C) HEK.hIP^{WT}, HEK.hIP^{SSLC}, HEK.hIP$^{\Delta383}$ or, as controls, HEK.TPα cells, each transiently transfected with pCMVTag2C:PDZK1^{FL}, were subject to immunoprecipitation with anti-HA 101R antibody. Immunoprecipitates (IP) were resolved by SDS–PAGE and immunoblotted (IB), as indicated. Uniform expression of Flag-tagged PDZK1 was verified by immunoblotting of whole cell lysates (50 μg/lane) with anti-FLAG antibody (bottom). The bar charts show mean relative levels of PDZK1-associated with the anti-HA 101R immunoprecipitates (relative protein, % ± SEM, n = 3) where levels associated with the anti-HA.hIP immunoprecipitates are expressed as 100%.

hIP domain (hIP$^{299–386}$ or hIP$^{320–386}$; Figure 1B, QDO). Conversely, PDZK1$^{1–154}$ did not interact with the internal hIP$^{299–320}$ subfragment, encoding the RBD only, or indeed with any of the controls including TPα$^{312–343}$, TPβ$^{312–407}$, p53 or the vector alone (Figure 1B, QDO). Furthermore, the interaction of PDZK1$^{1–154}$ with the hIP$^{299–386}$ or hIP$^{320–386}$ subfragments was independent of the presence of an isoprenylation 'Caa*X*' motif associated with the wild-type hIP (-C^{383}LSC; e.g., in hIP$^{299–386,WT}$ and hIP$^{320–386,WT}$) or an isoprenylation-defective variant (-S^{383}SLC; e.g., in hIP$^{299–386,SSLC}$ and hIP$^{320–386,SSLC}$) at its C terminus. In addition, consistent with previous reports, but distinct from that of PDZK1$^{1–154}$, Rab11a interacted only with subfragments containing an intact RBD, namely the hIP$^{299–386,WT/SSLC}$ and hIP$^{299–320}$subfragments (Reid *et al.*, 2010), whereas p53 interacted only with SV-40 large T antigen, which acted as an additional Y2H control (Figure 1B). Based on these data, PDZK1$^{1–154}$ specifically interacts with the C-tail domain of the hIP through an interaction that is not affected by mutation of its Caa*X* motif (-C^{383}LSC to -S^{383}LSC).

Thereafter, the ability of full-length PDZK1 (PDZK1$^{1–519}$, hereafter referred to as PDZK1) to interact with hemagglutinin (HA)-tagged forms of either the wild-type hIP, hIP^{SSLC}, or hIP$^{\Delta383}$ expressed in the previously characterized HEK.hIP, HEK.hIP^{SSLC}, and HEK.hIP$^{\Delta383}$ cell lines (Miggin *et al.*, 2003) was examined through coimmunoprecipitations. PDZK1 was detected in the anti-HA immunoprecipitates with both the wild-type hIP and isoprenylation defective hIP^{SSLC} and at similar levels in both cases (Figure 1C). In contrast, only trace amounts of PDZK1 was coimmunoprecipitated with the hIP$^{\Delta383}$ mutant devoid of its extreme four C-terminal residues including the entire Caa*X* motif (Figure 1C). PDZK1 was completely absent from the corresponding anti-HA:TPα immunoprecipitates from the control HEK.TPα cell line (Figure 1C). Such differences in the coimmunoprecipitation of PDZK1 with the HA-tagged receptors were not due to failure or variations of the immunoprecipitations per se or indeed due to differences in the levels of the Flag-tagged PDZK1 present in the cell lysates prior to immunoprecipitation (Figure 1C).

To further examine the possible influence of isoprenylation of the hIP on its interaction with PDZK1, the effect of inhibition of farnesylation of the hIP using the selective farnesyl transferase inhibitors (FTIs) R115777 and SCH66336 (O'Meara and Kinsella, 2004b, 2005) was examined. As a control for these studies, the ability of both FTIs to inhibit protein farnesylation was confirmed whereby they both efficiently inhibited farnesylation of

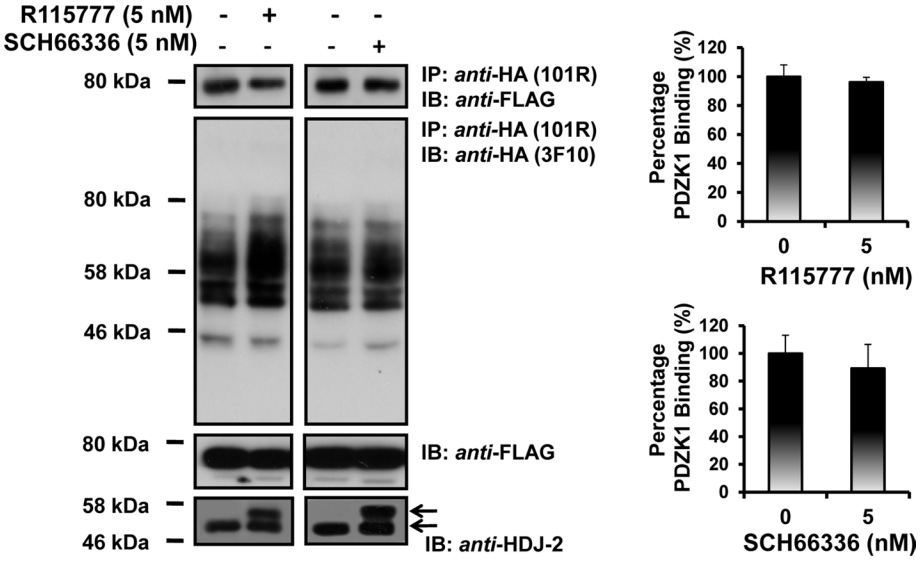

FIGURE 2. Effect of isoprenylation of the hIP on its interaction with PDZK1. HEK.hIP cells, transiently transfected with pCMVTag2C:PDZK1^{FL}, were preincubated with vehicle, R115777 (5 nM) or SCH66336 (5 nM) for 24 h prior to immunoprecipitation with anti-HA 101R antibody. Immunoprecipitates (IP) were resolved by SDS–PAGE and immunoblotted (IB), as indicated. Uniform expression of Flag-tagged PDZK1 was verified by immunoblot analysis of whole cell lysates (50 μg/lane) with anti-FLAG antibody (middle panels). The efficacy of R115777 or SCH66336 to inhibit protein farnesylation was validated by immunoblot analysis of whole cell lysates (50 μg/lane) for the farnesylated (~45–46 kDa) and nonfarnesylated (49 kDa) species of the molecular chaperone HDJ-2 (anti-HDJ-2; bottom panels). The bar charts show mean relative levels of PDZK1-associated with the anti-HA.hIP immunoprecipitates in the absence or of presence R115777 and SCH66336 (relative protein, % ± SEM, n = 3).

the molecular chaperone HDJ-2 as evidenced by the increased accumulation of its nonfarnesylated (49 kDa) in addition to its farnesylated (45 kDa) species (Figure 2, bottom panels) (O'Meara and Kinsella, 2004b). Moreover, neither R115777 nor SCH66336 FTIs affected the coimmunoprecipitation of PDZK1 with the hIP (Figure 2).

Collectively, these data identify a novel physical interaction between the hIP and PDZK1 in both yeast and mammalian cells. Although the interaction with PDZK1 requires the presence of the four C-terminal residues of the hIP, it is largely independent of the presence of a functional *–CaaX* motif or of the isoprenylation status of the hIP per se.

Characterization of the PDZ ligand within the hIP

PDZ domains have been described as protein interaction modules that recognize and bind the C-terminal residues (also termed the PDZ ligand) of their target protein(s) and, as stated, depending on their sequence composition can be broadly classified into Classes I–III (Tonikian *et al.*, 2008). Y2H-based approaches were used as a convenient means to characterize the putative PDZ ligand at the C terminus of the hIP, whereby the effect of mutation of residues at the 0 to −3 positions (hereafter defined as P_0, P_{-1}, P_{-2}, and P_{-3}; Figure 3) to corresponding Ser or Ala residues, either alone or in combination, was investigated. As previous, each of the bait and prey strains mated successfully (Figure 3, DDO). Specific mutation of residues at the P_{-3} (hIP$^{299–386,\underline{S}SLC}$) or P_{-1} (hIP$^{299–386,CS\underline{A}C}$, a variant not predicted to be isoprenylated; or hIP$^{299–386,CS\underline{S}C}$, a variant predicted to be isoprenylated) positions did not affect interaction of the hIP with PDZK1$^{1–154}$ (Figure 3). Conversely, mutation at the P_0 (hIP$^{299–386,CSL\underline{S}}$) abolished the interaction, whereas mutation at the P_{-2} (hIP$^{299–386,CA\underline{L}C}$) substantially reduced the interaction with PDZK1, suggesting that the C-terminal Cys^{386}, at P_0, and Ser^{384} at P_{-2} are specifically required for the interaction. Moreover, combined mutation of the $P_{0,-1,-2}$ (hIP$^{299–386,C\underline{AAA}}$), $P_{0,-1,-2,-3}$ (hIP$^{299–386,\underline{SAAA}}$), or deletion of $P_{0,-1,-2}$ (IP$^{299–386,C\text{-stop}}$ or hIP$^{299–386,S\text{-stop}}$) generated forms of the hIP that failed to interact with PDZK1$^{1–154}$ (Figure 3). Failure to detect an interaction was not due to altered/reduced expression of the various hIP$^{299–386}$-derived bait proteins, as confirmed by immunoblotting (Supplemental Figure 1). Collectively, these data reveal critical roles for the residues at P_0 and P_{-2}, but not at P_{-1} or P_{-3}, within the PDZ ligand of the hIP in defining its interaction with PDZK1 and thereby suggests that it can be classified as a class I type PDZ ligand.

Disruption of the GLGF motif within the PDZ domains of PDZK1

PDZK1 is a multi-PDZ domain adapter or scaffold protein containing four well-defined PDZ domains, hereafter referred to as PDZ^{D1}, PDZ^{D2}, PDZ^{D3}, and PDZ^{D4}, in addition to a short regulatory domain at its C terminus (Hu *et al.*, 2009; LaLonde and Bretscher, 2009). Although the initial Y2H screen identified PDZK1$^{1–154}$, corresponding to its entire PDZ^{D1} and only part of its PDZ^{D2}, as the region that interacts with the hIP, it was sought to investigate the specificity of the interaction of PDZ^{D1} and to establish whether any

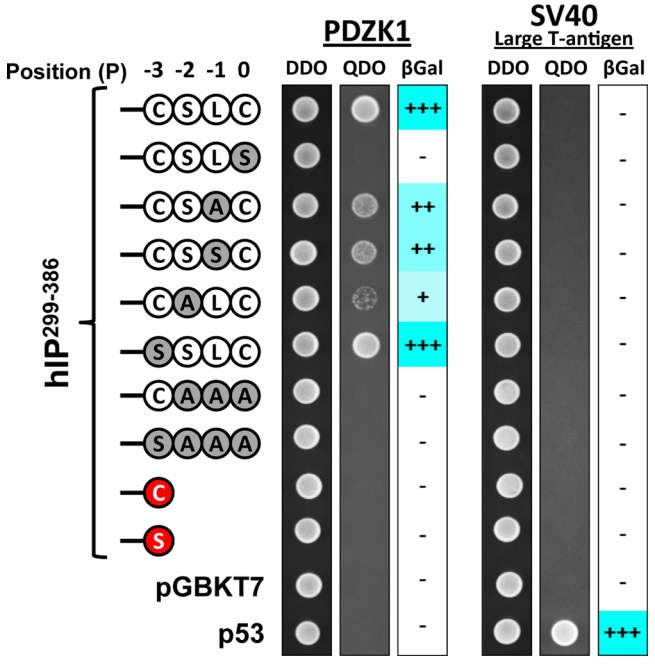

FIGURE 3. Characterization of the PDZ ligand within the C-tail domain of the hIP. *S.c* Y187 (pACT2:PDZK1) or, as a control, *S.c* Y187 (pTD1-1) prey strains were mated with *S.c* AH109 bait strains transformed with pGBKT7.hIP$^{299-386}$ subfragment with its wild-type (-C^{383}SLC^{386}, corresponding to the positions (P)$_0$, P_{-1}, P_{-2}, and P_{-3} of its PDZ ligand, respectively) carboxyl-terminal residues, or the listed mutated variants, and as controls, p53 or transformed with the vector pGBKT7 alone. Data: n ≥ 3.

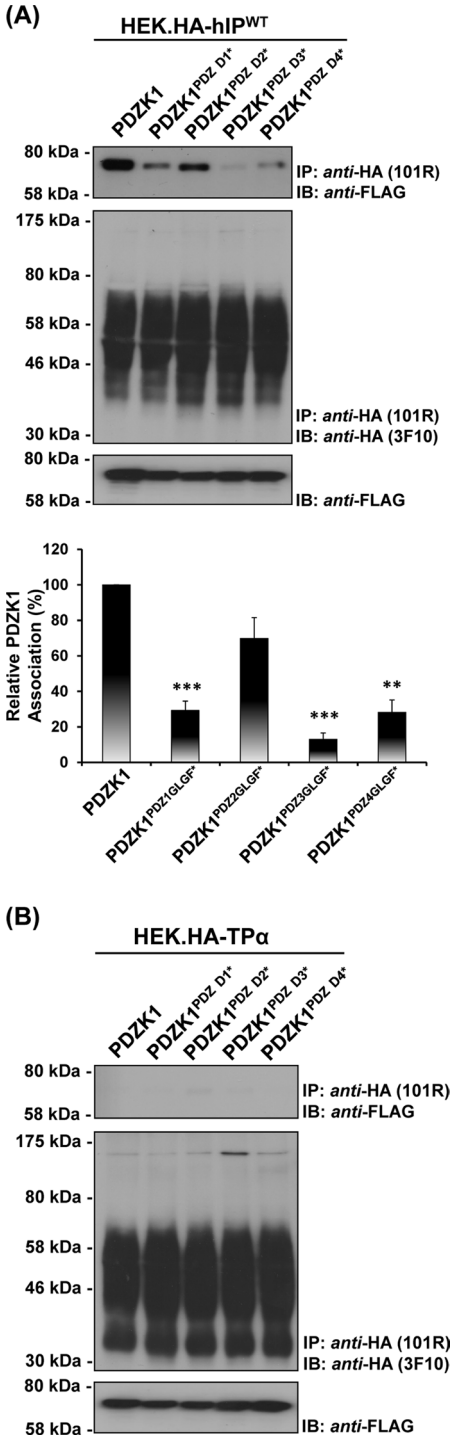

FIGURE 4. Identification of the PDZ domains involved in the interaction of PDZK1 with the hIP. HEK.hIP (A) or, as controls, HEK.TPα (B) cells, each transiently transfected with pCMVTag2C encoding FLAG-tagged PDZK1^{FL}, PDZK1^{PDZD1*}, PDZK1^{PDZD2*}, PDZK1^{PDZD3*}, or PDZK1^{PDZD4*}, were subject to immunoprecipitation with anti-HA 101R antibody. Immunoprecipitates (IP) were resolved by SDS–PAGE and immunoblotted (IB), as indicated. The bar charts show mean relative levels of the wild-type and mutated forms of PDZK1 associated with the anti-HA.hIP 101R immunoprecipitates (relative protein, % ± SEM, n = 3) where levels of the wild-type PDZK1 are expressed as 100%. The asterisks indicate where PDZK1 mutation resulted in significant reductions in complex associated PDZK1, where ** and *** indicate $p < 0.01$ and $p < 0.001$, respectively, for post hoc Dunnett's multiple comparison *t*-test analysis.

of the other PDZ domains, namely PDZ^{D2}, PDZ^{D3}, and PDZ^{D4}, may also contribute to the interaction with the hIP. Typically, mutation of the conserved hydrophobic GLGF motif within the carboxyl-binding loop/binding pocket of a given PDZ domain will disrupt interaction with its target PDZ ligand(s) and, hence, can be used experimentally to identify/validate specific PDZ protein:protein interactions (Lee and Zheng, 2010).

Herein mutation of the GLGF motif within PDZ^{D1} completely disrupted interaction of PDZK1$^{1–154}$ with each of the hIP$^{299–386}$-derived subfragments examined through Y2H-based studies (Supplemental Figure 1B). In agreement with previous data, in mammalian cells, full-length PDZK1 strongly and specifically coimmunoprecipitated with the wild-type hIP, but not with the control TPα, from their respective HEK.hIP and HEK.TPα stable cell lines (Figure 4, A and B). Whereas PDZK1^{PDZD2*}, carrying a mutated GLGF motif within PDZ^{D2}, appeared to coimmunoprecipitate along with the hIP at slightly reduced levels, statistical comparisons established that those levels were not significantly different from those of the wild-type PDZK1 ($P = 0.1439$). Conversely, the interactions of PDZK1^{PDZD1*} ($P < 0.001$) and PDZK1^{PDZD4*} ($P < 0.01$) with the hIP were substantially reduced, whereas the interaction of PDZK1^{PDZD3*} ($P < 0.001$) was almost completely abolished (Figure 4A). Moreover, none of the PDZK1 variants carrying the disrupted GLGF motifs within PDZ^{D1}, PDZ^{D2}, PDZ^{D3}, or PDZ^{D4} coimmunoprecipitated with TPα, a further endorsement of the specificity of the interaction between PDZK1 and hIP (Figure 4B). Furthermore, immunoblot analysis showed that differences in immunoprecipitation of PDZK1 or its GLGF motif variants were not due to differences in their expression levels or in the efficiency of the anti-HA immunoprecipitations per se (Figure 4, A and B, bottom and middle panels, respectively). Hence, collectively these data confirm a constitutive physical interaction between the hIP and PDZK1 in both yeast and mammalian cells and establish critical roles for PDZ^{D1}, PDZ^{D3}, and PDZ^{D4}, but not PDZ^{D2}, of PDZK1 in that interaction.

Effect of agonist activation of the hIP on its interaction with PDZK1

The selective IP agonist cicaprost (Kawabe *et al.*, 2010a) was used to investigate the possible influence of agonist activation of the hIP on its interaction with PDZK1. Consistent with previous data (Figure 1C), in the absence of agonist, PDZK1 showed a strong constitutive interaction with the hIP (Figure 5A). In response to cicaprost stimulation, the interaction of PDZK1 with the hIP was dynamically regulated in a time-dependent manner, for example, being significantly diminished at 10 min while returning to basal levels at 30–60 min and decreasing again at 2–4 h postagonist stimulation (Figure 5A). Differences in levels of PDZK1 associated with the immune complexes were not due to variations in the overall levels of PDZK1 expression or in the efficiency of the anti-HA immunoprecipitations (Figure 5A, bottom and middle panels, respectively).

PDZK1 has been established to undergo phosphorylation by cAMP-dependent PKA at Ser^{505} within its C-terminal regulatory region (Nakamura *et al.*, 2005). Furthermore, phosphorylation of PDZK1 by PKA at Ser^{505} critically regulates its interaction with many of its target proteins, including that of the HDL scavenger receptor SR-B1 (Nakamura *et al.*, 2005). Hence, to establish whether the observed dynamic interaction of PDZK1 with the hIP may involve agonist-regulated phosphorylation of PDZK1, the effect of cicaprost stimulation on the phosphorylation of PDZK1 was examined using anti-Phospho^{Ser} antibodies (Figure 5B). In the absence of agonist, PDZK1 was found to be basally or nett hypophosphorylated (Figure 5B). In response to cicaprost stimulation, the level

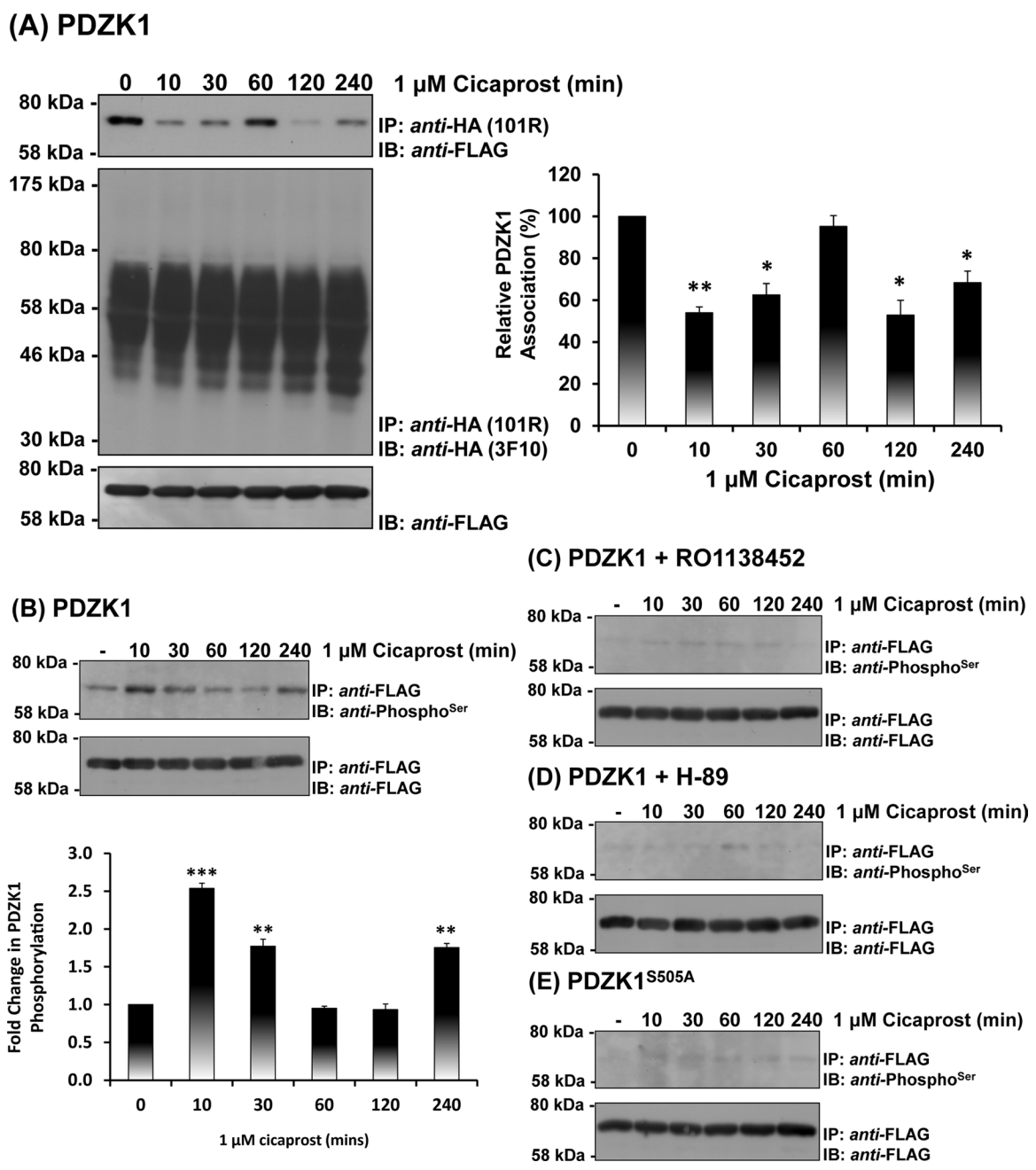

FIGURE 5. Effect of agonist activation of the hIP on the interaction and phosphorylation of PDZK1. (A) HEK.hIP cells, transiently transfected with pCMVTag2C:PDZK1, were stimulated with cicaprost (1 μM; 0–240 min). HA-tagged hIPs were immunoprecipitated with anti-HA 101R antibody; immunoprecipitates (IP) were resolved by SDS–PAGE and immunoblotted (IB), as indicated. The bar charts show mean relative levels of the PDZK1 associated with the anti-HA.hIP 101R immunoprecipitates as a function of cicaprost stimulation (relative protein, % ± SEM, n = 3) where levels in the absence of agonist are expressed as 100%. The asterisks indicate that cicaprost stimulation resulted in significant reductions in levels of PDZK1 associated with the hIP immune-complexes where * and ** indicate $p < 0.05$ and $p < 0.01$, respectively, for post hoc Dunnett's multiple comparison *t*-test analysis. (B–E) HEK.hIP cells, transiently transfected with either pCMVTag2C:PDZK1 (B–D) or pCMVTag2C:PDZK^{S505A} (E), were preincubated with vehicle (B, E), RO1138452 (10 μM; 10 min) (C), or H-89 (10 μM; 10 min) (D) prior to stimulation with cicaprost (1 μM; 0–240 min). Cells were then subject to immunoprecipitation with anti-FLAG antibody to immunoprecipitate PDZK1. Immunoprecipitates (IP) were resolved by SDS–PAGE and immunoblotted (IB), as indicated.

of PDZK1 phosphorylation was dynamically regulated, being substantially increased at 10–30 min post agonist stimulation (nett hyperphosphorylated) while returning to the basal, hypophosphorylated levels at 60– 120 min and increasing again, such as 240 min poststimulation (Figure 5B). Confirmation that the enhanced cicaprost-induced phosphorylation of PDZK1 is specifically mediated through activation of the hIP was established, whereby the selective IP antagonist RO1138452 (Clark *et al.*, 2004) blocked both basal and cicaprost-induced phosphorylation of PDZK1 (Figure 5C).

The hIP is primarily coupled to Gs-mediated activation of adenylyl cyclase leading to increases in cAMP concentrations and, in turn,

downstream activation of PKA (Lawler *et al.*, 2001b), whereas, as stated, PDZK1 has been established to undergo phosphorylation by PKA where Ser^{505} within its C-terminal regulatory region represents the critical phospho-target (Nakamura *et al.*, 2005). Herein it was established that preincubation with the PKA inhibitor H-89 also completely inhibited both basal and cicaprost-induced PDZK1 phosphorylation (Figure 5D). Furthermore, it was also established that the PDZK1 variant $PDZK1^{S505A}$ was not phosphorylated under basal conditions, in the absence of agonist, and did not undergo enhanced phosphorylation in response to cicaprost stimulation (Figure 5E). Differences in levels of phosphorylation of PDZK1, either in the absence or presence of cicaprost stimulation or in the presence of RO1138452 or H-89, or indeed phosphorylation of $PDZK1^{S505A}$, were not due to variations in the overall levels of PDZK1 or $PDZK1^{S505A}$ expression per se (Figure 5B–E, bottom panels). Hence, collectively these data demonstrate that PDZK1 constitutively interacts with the hIP but that the interaction is regulated in a transient and dynamic manner in response to agonist activation of the hIP. Furthermore, in the absence of agonist, PDZK1 is basally or hypophosphorylated but it undergoes enhanced cicaprost-induced phosphorylation in a transient, dynamic manner through a mechanism involving PKA phosporylation of PDZK1 at Ser^{505}.

Hence, to further investigate the role of Ser^{505} in contributing to the dynamic nature of the interaction of PDZK1 with the hIP, the effect of cicaprost stimulation on the interaction with both its phosphorylation-defective $PDZK1^{S505A}$ and phospho-mimetic $PDZK1^{S505D}$ variants was examined through coprecipitations. To begin, the interaction of $PDZK1^{S505A}$ and $PDZK1^{S505D}$, relative to that of the wild-type PDZK1, with the hIP was examined. In the absence of agonist, interaction of $PDZK1^{S505D}$ with the hIP was directly comparable to that of PDZK1 while the interaction between $PDZK1^{S505A}$ and the hIP was substantially reduced (Figure 6A, top panel). Furthermore, consistent with the phosphorylation data (Figure 5B–E), preincubation with two independent PKA inhibitors, namely H-89 and KT5720 (Davies *et al.*, 2000), substantially reduced with interaction of PDZK1 with the hIP, whereas preincubation with the protein kinase C (PKC) inhibitor GÖ6983 had no effect (Figure 6A). On the other hand, preincubation with H-89, KT5720, or GÖ6983 had no effect on the interaction of either $PDZK1^{S505A}$ or $PDZK1^{S505D}$ with the hIP in the absence of cicaprost (Supplemental Figure 2). In response to agonist activation, the interaction of $PDZK1^{S505A}$ with the hIP was completely lost at 10 min, and $PDZK1^{S505A}$ was not found in the anti-HA:hIP immune complexes even following sustained (4 h) cicaprost stimulation (Figure 6B, top panel). Conversely, the interaction of $PDZK1^{S505D}$ with the hIP was not regulated in response to agonist stimulation, remaining largely unaffected by cicaprost regardless of the incubation period (Figure 6C, top panel). As before, the observed differences in immunoprecipitation of PDZK1, $PDZK1^{S505A}$, and $PDZK1^{S505D}$ with the hIP were not due to differences in their levels of expression or in the efficiency of the anti-HA:hIP immunoprecipitations (Figure 6B and C, middle and bottom panels).

Hence, collectively these data confirm a constitutive interaction between the hIP and PDZK1 but that, in response to agonist activation, the interaction is modulated in a dynamic manner through a mechanism that is dependent, at least in part, on regulated PKA phosphorylation of PDZK1 at Ser^{505} in response to cicaprost stimulation.

Effect of PDZK1 on the expression and signaling of the hIP

Although PDZK1 has been shown to affect the level of expression and/or function of certain of its targets, such effects are protein and/or cell type–specific, as exemplified in the case of SR-B1 (Kocher and Krieger, 2009). Hence, herein, the effect of ectopic expression of PDZK1 on hIP expression levels and function was examined by immunoblot and flow cytometry analyses and through assessment of its radioligand binding and agonist-induced cAMP generation (Figure 7 and Supplemental Figure 3). Although immunoblot analysis suggested that PDZK1 did not affect overall IP expression levels, radioligand binding assays (RLBAs) established that ectopic expression of PDZK1 resulted in a 1.5-fold increase in binding of its selective radioligand [^{3}H]iloprost in crude membrane preparations ($P < 0.001$; Figure 7A, 30°C). Immunofluorescence image analyses also confirmed that the hIP and PDZK1 show some degree of colocalization, particularly at cell membranes, but there was no detectable change in the overall level of hIP expression following ectopic expression of PDZK1 (Supplemental Figure 3C; and data not shown). To assess whether the increase in [^{3}H]iloprost binding in the presence of PDZK1 is actually due to alterations in the levels of the hIP at the cell surface, RLBAs were also carried out at 4°C on whole cells, as opposed to at 30°C, thereby blocking any internalization of the ligand-bound receptor complex (Figure 7A). Consistent with the radioligand binding on membrane preparations, overexpression of PDZK1 led to similar increases in [^{3}H]iloprost binding and, hence, suggested that PDZK1 enhances hIP expression at the cell surface ($P < 0.001$; Figure 7A, 4°C). These findings were also corroborated by flow cytometric analysis, whereby the relative fluorescence intensity due to anti-HA hIP expression was increased ~1.4-fold in the presence of overexpressed PDZK1 (Supplemental Figure 3, A and B).

Furthermore, overexpression of PDZK1 resulted in a significant increase in cicaprost-induced cAMP generation in HEK 293 cells (Figure 7B). Disruption of the GLGF domains in PDZ^{D1} and PDZ^{D3}, but not PDZ^{D2} or PDZ^{D4}, of PDZK1 completely abrogated these effects, further implicating an involvement of both PDZ^{D1} and PDZ^{D3} in the specific interaction with the hIP (Figure 7, C and D; also see Figure 4B). More specifically, similar to wild-type PDZK1, ectopic expression of $PDZK1^{PDZD2*}$ and $PDZK1^{PDZD4*}$ resulted in significant increases in both [^{3}H]iloprost binding and agonist-induced cAMP generation, whereas overexpression of $PDZK1^{PDZD1*}$ and $PDZK1^{PDZD3*}$ had no effect. Furthermore, immunoblotting confirmed equivalent expression of PDZK1 and its variants and, hence, that the observed effects on functional expression of the hIP were not due to variations in PDZK1 expression levels (Figure 7, C and D). Combined, these data show that increased expression of PDZK1 leads to enhanced functional expression of the hIP at the plasma membrane, resulting in its increased radioligand ([^{3}H]iloprost) binding and agonist-induced cAMP generation. Additionally, PDZ domains 1 and 3, but not 2 and 4, were shown to be critical for the ability of PDZK1 to mediate these effects.

Effect of PDZK1 on cicaprost-induced endothelial cell migration and angiogenesis

Both the hIP and PDZK1 are expressed within the vascular endothelium, where they are individually functionally important, not least through their aforementioned regulation of endothelial cell migration and/or angiogenesis (Zhu *et al.*, 2008; Kawabe *et al.*, 2010b). Hence, as an initial means of exploring the functional significance of the interaction in a more physiologically relevant setting, the interaction between the hIP and PDZK1 was investigated in primary human umbilical vein endothelial cells (1° HUVECs). PDZK1 was detected in immune complexes with the hIP from 1° HUVECs (Supplemental Figure 4A), where immunoprecipitations were performed using an affinity-purified antibody directed to the intracellular loop $(IC)_2$ domain of the hIP (Turner and Kinsella, 2010). PDZK1

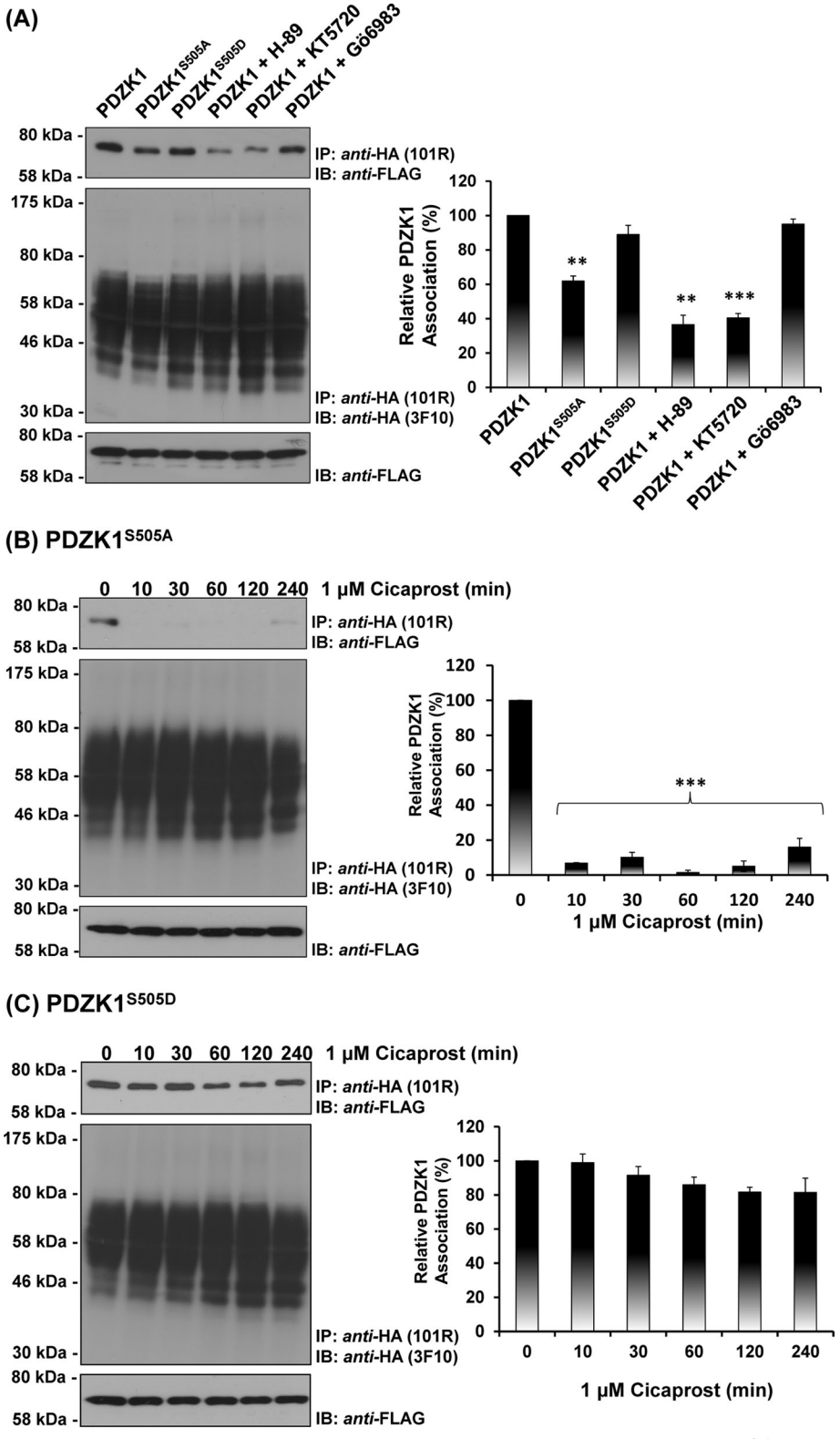

FIGURE 6. Effect of agonist activation of the hIP on its interaction with PDZK1, PDZK1^{S505A}, and PDZK1^{S505D}. (A) HEK.hIP cells, transiently transfected with pCMVTag2C encoding PDZK1, PDZK1^{S505A}, or PDZK1^{S505D}, were incubated with vehicle (0.01% DMSO; 10 min), H-89 (10 μM; 10 min), KT5720 (5 μM; 10 min), or GÖ6983 (1 μM; 10 min), as indicated. Alternatively, HEK.hIP cells, transiently transfected with pCMVTag2C encoding PDZK1^{S505A} (B) or PDZK1^{S505D} (C), were stimulated with cicaprost (1 μM; 0–240 min). HA-tagged hIPs were immunoprecipitated with anti-HA 101R antibody; immunoprecipitates (IP) were resolved by SDS–PAGE and immunoblotted (IB), as indicated. The bar charts show mean relative levels of the PDZK1, PDZK1^{S505A}, and PDZK1^{S505D} -associated with the anti-HA.hIP 101R immunoprecipitates as a function of cicaprost stimulation (relative protein, % ± SEM, n = 3) where levels in the absence of agonist are expressed as 100%. The asterisks indicate that inhibiton of PKA (A) or cicaprost stimulation (B, C) resulted in significant reductions in PDZK1 levels in anti-HA immunoprecipitates, where ** and *** indicate p = 0.01 and p = 0.001, respectively, for post hoc Dunnett's multiple comparison *t*-test analysis.

was not present in the precipitate employing the control preimmune immunoglobulin (Ig)G, and failure to detect PDZK1 in the preimmune complex was not due to differences in its expression levels (Supplemental Figure 4A).

As stated, the IP has also been implicated in endothelial cell migration (Pola *et al.*, 2004) and angiogenesis (Kawabe *et al.*, 2010b), and studies herein demonstrate a highly specific interaction between the hIP and PDZK1. Therefore it was sought to investigate prostacyclin-induced endothelial cell migration and angiogenesis and, more specifically, to examine the possible influence of PDZK1 on those effects, where studies involving HDL/SR-B1 and vascular endothelial growth factor (VEGF) acted as reference controls. PDZK1, through its interaction with SR-B1, is known to play a critical role in HDL-mediated endothelial cell migratory and angiogenic responses, whereas such VEGF-mediated responses are entirely independent of PDZK1 (Zhu *et al.*, 2008) (see Figure 9B later in the paper). Stimulation of 1° HUVECs with the selective IP agonist cicaprost led to significant increases in endothelial cell migration, an effect completely abrogated by the IP antagonist RO1138452 (Figure 8Ai). Consistent with numerous studies, VEGF and HDL also promoted endothelial cell migration, which was further augmented by cicaprost costimulation (Figure 8Aii and Aiii; P = 0.04 and P = 0.015, respectively, by two-way analysis of variance [ANOVA]). Collectively, these data reveal a specific role for the hIP in promoting basal-, VEGF-, and HDL-mediated migration of 1° HUVECs.

To investigate the role of PDZK1 in migration of 1° HUVECs, small interfering RNA (siRNA) was used to disrupt its expression in 1° HUVECs (Figure 8D). Consistent with previous reports (Zhu *et al.*, 2008), it was confirmed that targeted knockdown of PDZK1 using siRNA$_{PDZK1}$, but not the scrambled control siRNA$_{CONTROL}$, almost completely abrogated HDL-mediated cell migration in 1° HUVECs (Figure 8C) and also resulted in small, but significant, reductions in basal migration (Figure 8C, and

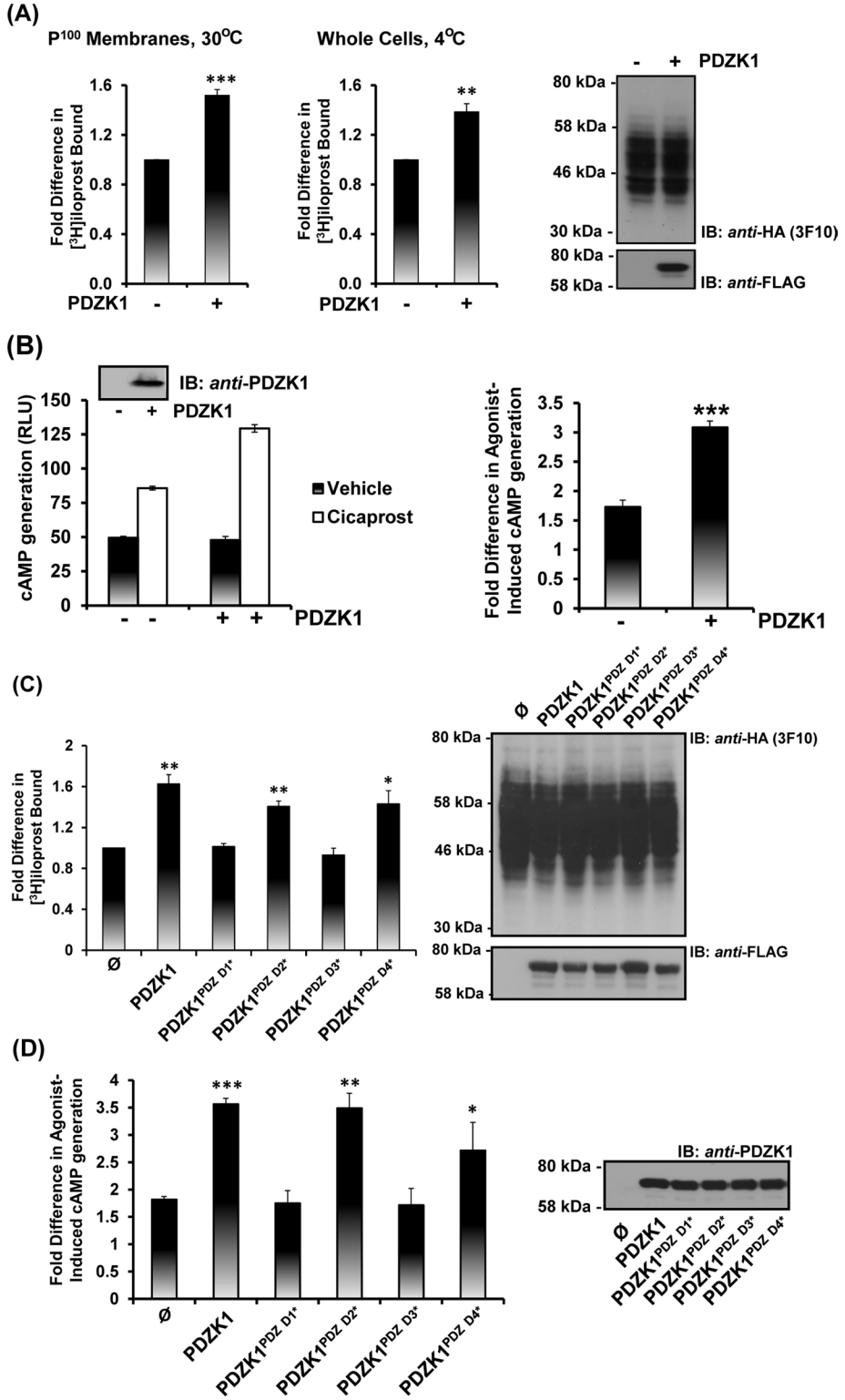

FIGURE 7. Effect of PDZK1 on the expression and signaling of the hIP. (A, C) HEK.hIP cells were transiently transfected with pCMVTag2C encoding either PDZK1 (A) or PDZK1, PDZK1$^{PDZ\ D1*}$, PDZK1$^{PDZ\ D2*}$, PDZK1$^{PDZ\ D3*}$, and PDZK1$^{PDZ\ D4*}$ or, as controls, pCMVTag2C vector (ø) alone (C). RLBA was performed 72 h posttransfection in the presence of 4 nM [^{3}H]iloprost for 60 min using either crude membrane (P_{100}) fractions (30°C; A, C) or whole cells (4°C; A). Data are presented as fold increases in [^{3}H]iloprost bound as a function of PDZK1 expression where levels in the presence of wild-type PDZK1 are expressed as 1. (B, D) HEK 293 cells were transiently cotransfected with pHM6:hIP, pADVA, pCRE-LUC, and pRL-TK in the presence of pCMVTag2C encoding PDZK1^{FL} (B) or PDZK1^{FL}, PDZK1$^{PDZ\ D1*}$, PDZK1$^{PDZ\ D2*}$, PDZK1$^{PDZ\ D3*}$, and PDZK1$^{PDZ\ D4*}$ or, as controls, pCMVTag2C vector (ø) alone (D). Cells were incubated with either vehicle or cicaprost (1 μM; 3 h) prior to determination of cAMP generation (RLU ± SEM; n = 3), where data are represented as levels of agonist-induced cAMP generation (B, left bar charts) and as fold inductions in agonist-induced cAMP accumulation (B, right bar charts; and D). Expression of the HA-tagged hIP and Flag-tagged PDZK1 proteins were verified by immunoblot analysis of the respective whole-cell lysates (50 μg/lane), as indicated. The asterisks indicate where ectopic expression of PDZK1 resulted in significant fold increases in [^{3}H]iloprost bound (A, C) or agonist-induced cAMP accumulation (B, D) where *, **, and *** indicate $p < 0.05$, $p < 0.01$, and $p < 0.001$, respectively, for post hoc Dunnett's multiple comparison *t*-test analysis. Levels of [^{3}H]iloprost binding in HEK.hIP cells were 1.1 ± 0.04 pmol/mg of cell protein (n = 4). Basal levels cAMP generation in HEK.hIP cells was 0.70 ± 0.04 pmol/mg of cell protein (n = 4) and was not affected by ectopic expression of PDZK1 or its mutated variants.

Supplemental Figure 4B). In contrast, the effect of siRNA$_{PDZK1}$ on VEGF-mediated migration was not significantly different from its effect on basal migration (Figure 8C), confirming that PDZK1 does not influence or participate in VEGF migration. In contrast to this, targeted disruption PDZK1 by siRNA$_{PDZK1}$ completely inhibited cicaprost-induced cell migration in 1° HUVECs, whereas the siRNA$_{CONTROL}$ (Figure 8C) or siRNA$_{LAMIN\ A/C}$ (data not shown) had no effect.

The influence of the interaction between hIP and PDZK1 on endothelial tube formation, a further essential step in the angiogenic process, was also investigated. In the presence of cicaprost, there was a significant increase in mean tube length (Figure 8B), an effect completely abrogated by coincubation with the IP antagonist RO1138452 (Figure 8B). Stimulation with both VEGF and HDL led to significant increases in mean tube lengths, and costimulation with cicaprost further enhanced both these effects (Figure 8B; P = 0.043 and P = 0.02, respectively, by two-way ANOVA). Similar to the findings for endothelial cell migration, while targeted disruption of PDZK1 with siRNA$_{PDZK1}$ led to small, but significant, reductions in basal tube formation in the absence of stimulation (Supplemental Figure 4C), it did not lead to further reductions in VEGF-induced migration (Figure 8E). In contrast, and consistent with our migration data (Figure 8C), disruption of PDZK1 expression impaired HDL-mediated endothelial tube formation (Figure 8E). Furthermore, targeted disruption of

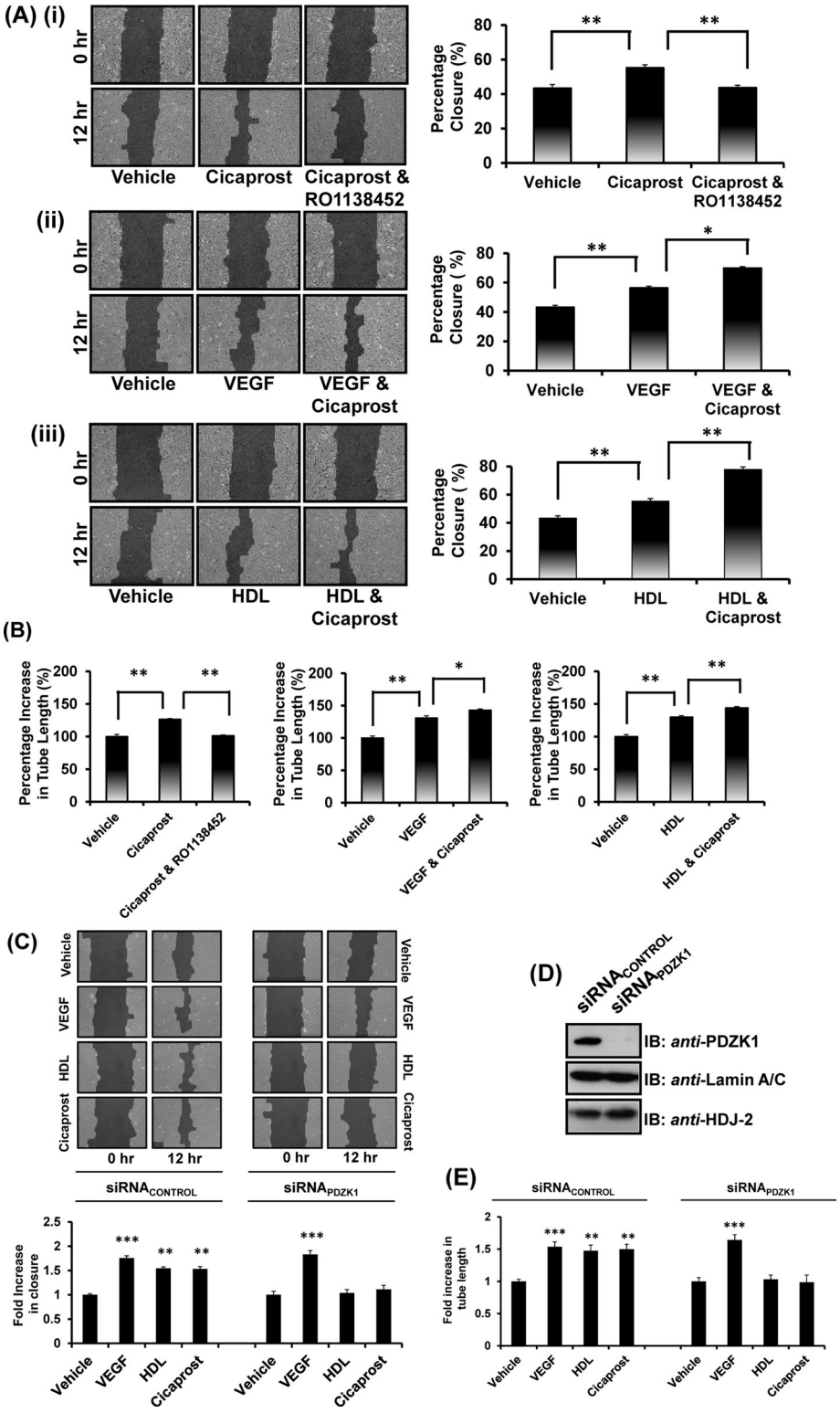

FIGURE 8. Effect of PDZK1 on hIP agonist-induced migration and endothelial tube formation in 1° HUVECs. (A, B) Migration after scratch wounds in 1° HUVEC monolayers (A) or tube formation of HUVECs seeded on Matrigel (B) in the presence of cicaprost (1 μM), VEGF (50 ng/ml), or HDL (50 μg/ml), alone or in combination and in the absence or presence of RO1138452 (10 μM; 10 min preincubation) were analyzed at 12 h. Bar charts represent mean percentage closure (% ± SEM; n = 3) at 12 h (A) or mean percentage of basal tube length at 12 h (% ± SEM; n = 3) (B). (C–E) 1° HUVECs were transfected with $siRNA_{PDZK1}$ or $siRNA_{control}$, where immunoblot analysis confirmed specific disruption of PDZK1 expression (D). Migration (C) and tube formation (E) was analyzed in the presence of vehicle, VEGF, HDL or cicaprost, as indicated, at 0 h and 12 h. Bar charts represent mean fold increases (± SEM; n = 3) in either wound closure or tube length in the presence of vehicle, VEGF, HDL or cicaprost, as indicated, at 12 h. The asterisks indicate either significant agonist-induced increases in migration (A), significant agonist-induced increases in tube length (B), significant fold increases in agonist-induced migration in comparison to vehicle-treated cells (C), significant fold increases in agonist-induced tube length in comparison to vehicle-treated cells (E) where *, **, and *** indicate $p < 0.05$, $p < 0.01$, and $p < 0.001$, respectively, for post hoc Dunnett's multiple comparison *t*-test analysis.

PDZK1 by $siRNA_{PDZK1}$ also completely inhibited cicaprost-induced endothelial tube formation in 1° HUVECs, whereas the $siRNA_{CONTROL}$ (Figure 8E) or $siRNA_{LAMIN\ A/C}$ (data not shown) had no effect.

Taken together, these data confirm an important role for the hIP in endothelial cell migration and in promoting angiogenesis through endothelial tube formation in vitro. Furthermore, and similar to that previously found to occur for HDL/SR-B1, they establish a critical role for PDKZI in mediating both cicaprost/IP-induced endothelial migration and in vitro angiogenesis. Collectively, the data presented herein identify a novel physical interaction between the hIP and the intracellular adapter protein PDZK1 that impacts on hIP-mediated endothelial function and sheds critical new insights into knowledge of the interplay between the hIP, but also of PDZK1 and HDL/SR-B1, as key players in the maintenance of endothelial monolayer integrity.

DISCUSSION

In this study, we report the discovery of a novel interaction between the hIP with PDZK1, a member of the NHERF family of PDZ domain-containing scaffolding proteins (Hu *et al.*, 2009; Kocher and Krieger, 2009). The direct interaction occurs through binding of a class I type PDZ ligand at the C terminus of the hIP with the domains PDZ^{D1}, PDZ^{D3}, and PDZ^{D4} of PDZK1. The ability of the hIP to bind several PDZ domains is consistent with the binding preferences of certain other proteins to bind PDZK1 and is, for example, identical to CFTR in that they both bind PDZ^{D1}, PDZ^{D3}, and PDZ^{D4} but not PDZ^{D2} (Wang *et al.*, 2000). As stated, the hIP is somewhat unusual among GPCRs in that it undergoes isoprenylation within a conserved carboxyl terminal -$C^{383}SLC^{386}$, or 'CaaX' motif (Hayes *et al.*, 1999; Miggin *et al.*, 2002), whereas data herein establish that this sequence also serves as a PDZ ligand. Such an interaction of an isoprenylated protein with PDZ domain proteins

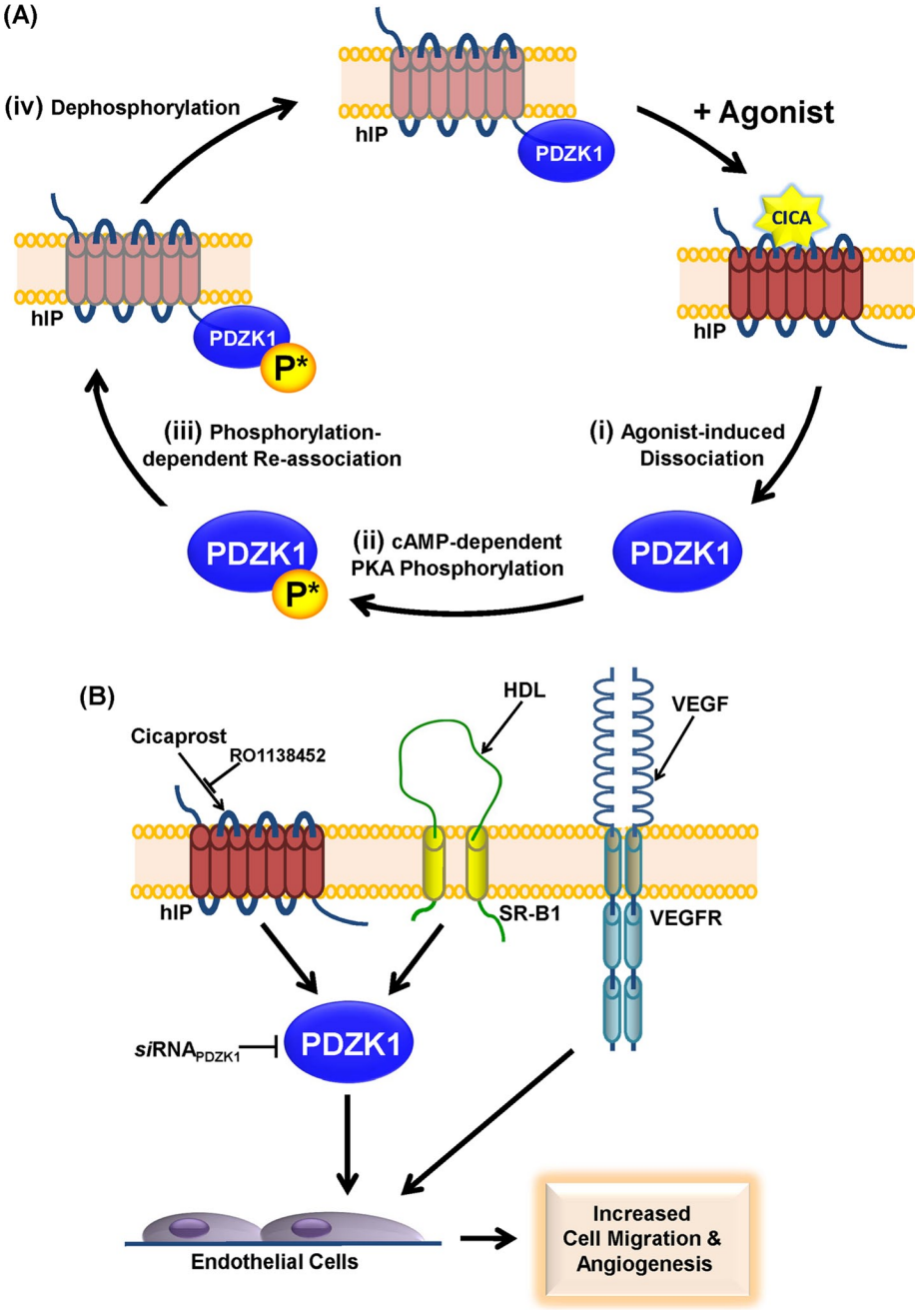

FIGURE 9. Proposed model of the interaction of PDZK1 with the hIP and its implications for endothelial cell migration and in vitro angiogenesis. (A) In the absence of agonist, PDZK1 is constitutively associated in a complex with the hIP, where PDZK1 is either not phosphorylated or basally hypophosphorylated. On cicaprost stimulation, (i) the hIP undergoes an agonist-induced conformational activation leading to dissociation of PDZK1. (ii) Released PDZK1 is then subject to enhanced hIP induced cAMP-dependent PKA phosphorylation at Ser^{505}, and (iii) this enhanced or nett hyperphosphorylated PDZK1 triggers its reassociation with the hIP. The reassociation of PDZK1 and hIP is coincident with regulated (iv) dephosphorylation of PDZK1 and its return to basal or hypophosphorylated levels. Consistent with this model, the phospho-defective $PDZK1^{S505A}$ is found in a constitutive complex with the hIP and undergoes agonist-induced dissociation but cannot undergo phosphorylation-induced reassociation in response to receptor activation. In contrast, the phospho-mimetic $PDZK1^{S505D}$ is hypothesized to mimic the hyperphosphorylated protein state (state iii), whereby any transient agonist-induced dissociation in the interaction of this mutant with the hIP is immediately recovered due to it mimicking the hyperphosphorylated state. (B) Agonist activation of the hIP, SR-B1, and VEGFR leads to enhanced endothelial cell migration and tube formation/in vitro angiogenesis. Consistent with a previous study (Zhu *et al.*, 2008), HDL/SR-B1-, but not VEGF/VEGFR-, mediated endothelial cell migration is dependent on its interaction with PDZK1. Herein it was established that, similar to that of HDL/SR-B1, cicaprost activation of the RO1138452-sensitive hIP promotes endothelial cell migration and tube formation and that these effects are dependent on PDZK1. siRNA disruption of PDZK1 inhibits both cicaprost- and HDL-, but not VEGF-, induced endothelial cell responses.

described herein for the hIP is not without precedence, being exemplified by the interaction of Gγ13 with PSD95, Veli-2, and SAP97 involving classic PDZ domain:PDZ ligand type interactions (Li *et al.*, 2006). Furthermore, while several lines of evidence herein suggest that the interaction of PDZK1 with the hIP is largely independent of its isoprenylation status, additional follow-up studies involving more direct biophysical approaches are required to ascertain whether the farnesylated, fully processed form of the hIP actually interacts with PDZK1.

Agonist activation plays an important role in regulating the signaling pathways of members of the GPCR superfamily, including the hIP (Lawler *et al.*, 2001b; O'Keeffe *et al.*, 2008; Wikstrom *et al.*, 2008; Reid *et al.*, 2010). The ability of PDZK1 to regulate the expression of the high-affinity HDL SR-B1 receptor is subject to functional regulation by phosphorylation, whereby cAMP-dependent PKA phosphorylation of Ser^{505} within the C-terminal regulatory region of PDZK1 is the critical phosphorylation event (Nakamura *et al.*, 2005). Herein several lines of evidence suggest that PDZK1 may also undergo PKA phosphorylation at Ser^{505} in response to cicaprost activation, which in turn may provide a molecular basis for the observed agonist-regulated dynamic interaction between PDZK1 and the hIP. Based on data presented in Figures 5 and 6, a model presented in Figure 9A proposes that PDZK1 is recruited into a complex with the hIP in a basal nonphosphorylated or overall nett hypophosphorylated state at Ser^{505}. In response to cicaprost-induced receptor activation, while (i) PDZK1 dissociates from the hIP complex, it also undergoes enhanced (ii) cAMP dependent-PKA phosphorylation at Ser^{505}, which, in time, (iii) triggers reassociation of PDZK1 with the hIP followed by (iv) dephosphorylation of PDZK1 to basal levels (Figure 9A). Evidence for the model is substantiated by the finding that the phosphorylation-defective variant $PDZK1^{S505A}$ interacts, albeit weaker than PDZK1, with the hIP under basal conditions and dissociates from the complex in response to agonist activation of the hIP. However, unlike wild-type PDZK1, the mutant $PDZK1^{S505A}$ cannot undergo

cicaprost-induced PKA phosphorylation and therefore does not undergo phosphorylation-induced reassociation with the hIP. Furthermore, and in contrast to this, it is proposed that the mutant PDZK1^{S505D} mimics the hyperphosphorylated state (iii). Hence, while it is possible that PDZK1^{S505D} may undergo dissociation in response to agonist activation of the hIP, such effects are not observed using the experimental approaches used in the current study, at least. By mimicking the hyperphosphorylated state, it is proposed that any dissociation of PDZK1^{S505D} would be followed by its rapid recruitment into the complex with the hIP, therefore leading to the observed stabilized or prolonged interaction of PDZK1^{S505D} with the hIP either in the absence or presence of agonist activation (Figure 9A, iii). Whereas certain aspects of the agonist-dependent regulation of PDZK1 with the hIP remain to be elucidated, including (a) whether PDZK1 is phosphorylated or not at Ser^{505} when bound to the hIP under basal conditions, (b) the identity of the phosphatase(s) that regulate the dephosphorylation of PDZK1, and (c) the nature of the agonist-induced conformational trigger(s) that promotes the dissociation at the level of the hIP itself, regulation of PDZ interactions by phosphorylation is not confined to PDZK1/NHERF3 (Voltz *et al.*, 2007). Critically, data herein now also establish that agonist activation of the hIP leads to direct PKA phosphorylation of PDZK1 to modulate their interaction, and it will be of interest to establish whether hIP-mediated phosphorylation of PDZK1 modulates its interaction with other targets, such as the SR-B1 or CFTR.

In contrast to the quite rapid temporal association and dissociation between the hIP and PDZK1, the hIP has also been established to undergo internalization and subsequent recyclization to the plasma membrane in response to agonist stimulation, but such events are much slower, occur maximally at 2–4 h post agonist stimulation (O'Keeffe *et al.*, 2008; Wikstrom *et al.*, 2008; Reid *et al.*, 2010). Hence, the temporal association and dissociation of PDZK1 with the hIP is a much more dynamic event, being largely regulated by phosphorylation/dephosphorylation, whereas the agonist-induced internalization of the hIP is a much slower event, requiring engagement and participation of the intracellular trafficking machinery, including members of the Rab GTPases, as we have previously reported (O'Keeffe *et al.*, 2008; Wikstrom *et al.*, 2008; Reid *et al.*, 2010). Therefore, it is unlikely that there is a relationship between the temporal association between the hIP with PDZK1 and the processes regulating agonist-induced trafficking of the hIP. Although PDZK1 has been shown to affect the level of expression and/or function of certain of its targets, such effects are protein and/or cell type–specific (Kocher *et al.*, 2003; Zhu *et al.*, 2008). PDZK1 does not substantially regulate overall expression of the hIP, in the cell type examined at least, but led to increased functional expression of the hIP at the cell surface, enhancing ligand binding and cAMP generation. Although disruption of the GLGF motif within PDZ^{D1} and PDZ^{D3} abrogated these effects, disruption of PDZ^{D4} did not appear to be functionally important, despite its ability to influence the interaction of PDZK1 with the hIP.

By binding to its C-terminal PDZ ligand, PDZK1 plays an essential role in maintaining hepatic SR-BI levels, thereby controlling HDL metabolism/reverse cholesterol transport and HDL/SR-BI–dependent endothelial cell migration, tube formation, and proliferation, protecting against the development of atherosclerosis (Fenske *et al.*, 2008, 2009; Zhu *et al.*, 2008). PDZK1$^{-/-}$ mice display marked hypercholesterolaemia due to a 95% decrease in hepatic SR-B1 expression and thereby represent an important preclinical model of CV disease (Kocher and Krieger, 2009). Furthermore, although PDZK1 does not influence SR-B1 levels within the vascular endothelium, PDZK1$^{-/-}$ mice also impaired EC migration/re-endothelialization, contributing to decreased vascular repair and increased atherosclerosis (Zhu *et al.*, 2008). Hence, through its interaction with SR-B1, PDZK1 is critically involved in maintaining endothelial monolayer integrity. In contrast, PDZK1 does not influence endothelial cell migration or angiogenesis by VEGF, and therefore it was suggested that it is uniquely required for signaling by HDL/SR-B1 within the endothelium (Zhu *et al.*, 2008).

Categorical evidence of the importance of prostacyclin to vascular repair and angiogenesis was recently demonstrated whereby regenerative endothelial progenitor cells (EPCs) from IP$^{-/-}$ mice failed to promote re-endothelialization, highlighting a critical protective role for the IP in vascular remodeling in response to injury similar to that of the HDL/SR-B1–mediated pathway (Qu *et al.*, 2009; Kawabe *et al.*, 2010b). In the current study, as outlined in the model in Figure 9B, it was established that PDZK1 also plays a critical role in IP-mediated endothelial cell migration and in vitro angiogenesis (Figure 8). Although a number of studies have suggested that prostacyclin-induced endothelial migration and angiogenesis occurs through its regulation of PPARδ, rather than through the IP per se (Pola *et al.*, 2004; He *et al.*, 2008), those studies used iloprost as agonist, which, unlike the highly selective IP agonist cicaprost used herein, is known to activate both the IP and PPARδ (Kawabe *et al.*, 2010a). Moreover, in the current study, the effects of cicaprost were blocked by the IP antagonist RO1138452 and by targeted knockdown of PDZK1 using siRNA$_{PDZK1}$. Taken together, our findings establish a specific and critical role for the hIP in modulating endothelial migratory and angiogenic responses and, similar to the HDL/SR-B1 pathway, that those agonist-induced responses are PDZK1-dependent (Figure 9B). Considering the central role of the hIP and SR-B1 within the vasculature, including re-endothelialization in response to injury, coupled with the finding herein of a direct interaction of PDZK1 with the hIP, it will be of significant interest to investigate the possible interplay between the critical prostacyclin/IP and HDL/SR-B1 pathways, both of which are now known to be critically regulated by PDZK1.

MATERIALS AND METHODS

Materials

Cicaprost was obtained from Schering AG (Berlin, Germany). RO1138452 was obtained from Cayman Chemicals (Ann Arbor, MI); H-89, KT5720, and GÖ6983 were from Merck Biochemicals (Darmstadt, Germany). Mouse monoclonal anti-HA 101R antibody was from Cambridge Biosciences (Cambridge, UK); mouse polyclonal anti-PDZK1, normal rabbit IgG, horseradish peroxidase (HRP)-conjugated goat anti–rabbit and goat anti–mouse secondary antibodies were from Santa Cruz Biotechnology (Santa Cruz, CA); rat monoclonal anti-HA 3F10-HRP–conjugated antibody was from Roche (Nutley, NJ); anti-Myc (9B11) mouse mAb was from Cell Signaling Technology (Beverly, MA); rabbit anti-PhosphoSer antibody was from Invitrogen (61–8100; Carlsbad, CA); recombinant human vascular endothelial growth factor (VEGF) 165 (293-VE/CF) was from R&D Systems (Minneapolis, MN); HDL (purified from human plasma; L1567), mouse monoclonal anti-FLAG and anti-FLAG-HRP–conjugated M2 antibody were from Sigma-Aldrich (St. Louis, MO); anti-HDJ-2 (DNAJ protein) was from NeoMarkers (Fremont, CA); AlexaFluor488 goat anti–rabbit, AlexaFluor488 goat anti–mouse, and AlexaFluor594 goat anti–mouse antibodies were from Molecular Probes (Eugene, OR). Plasmids pCRE-Luc, pRL-TK, and pCMVTag2C were from Agilent Technologies (Santa Clara, CA). Farnesyl transferase inhibitors R115777 and SCH66336 were obtained from Janssen Pharmaceuticals (Titusville, NJ) and Schering-Plough (Kenilworth, NJ),

respectively. [^{3}H]iloprost was obtained from Perkin Elmer (Waltham, MA). All oligonucleotides were synthesised by Sigma Genosys.

Subcloning and site-directed mutagenesis

The plasmids pHM6:hIP^{WT}, pHM6:hIP^{SSLC}, and pHM6:hIP$^{\Delta383}$, encoding HA epitope-tagged forms of the wild-type hIP, isoprenylation defective hIP^{SSLC}, or Caa*X*-truncated hIP$^{\Delta383}$, respectively, have been previously described (Hayes *et al.*, 1999). pACT2:Rab11a, pGBKT7:hIP$^{299–386}$, pGBKT7:hIP$^{299–386,SSLC}$, pGBKT7:hIP$^{320–386}$, pGBKT7:hIP$^{320–386,SSLC}$, and pGBKT7:hIP$^{299–320}$ have been described (Wikstrom *et al.*, 2008). The plasmids pGBKT7:TP$\alpha^{312–343}$ and pGBKT7:TP$\beta^{312–407}$ have also been described (Reid *et al.*, 2011). The plasmids pGBKT7:hIP$^{299–386,CSLS}$, pGBKT7:hIP$^{299–386,CSAC}$, pGBKT7:hIP$^{299–386,CSSC}$, pGBKT7:hIP$^{299–386,CALC}$, pGBKT7:hIP$^{299–383,C\text{-}STOP}$, pGBKT7:hIP$^{299–383,S\text{-}STOP}$, pGBKT7:hIP$^{299–386,CAAA}$, and pGBKT7:hIP$^{299–386,SAAA}$ were generated by subcloning the respective region of the wild-type or mutant hIP from the corresponding pHM6-based plasmids into the *Eco*RI–*Bam*HI sites of the yeast bait vector pGBKT7 (Clontech, Mountain View, CA), such that fragments were in-frame with the DNA-binding domain (DBD) of the yeast GAL4 transcriptional activator. The plasmid pACT2:PDZK1^{PDZD1*} was generated by QuikChange site-directed mutagenesis (Agilent Technologies) using the PDZK1 library clone identified in the Y2H screen, pACT2:PDZK1, as template and the primer pair shown in Supplemental Table 1. The plasmid pOBT7:PDZK1 was obtained from Source BioScience imaGenes (Berlin, Germany), and the plasmid pCMVTag2C:PDZK1 was generated by subcloning the full-length sequence from pOBT7:PDZK1 into the *Bam*HI–*Xho*I sites of the mammalian expression vector pCMVTag2C, such that fragment was in-frame for FLAG epitope-tagged protein expression. The plasmids pCMVTag2C:PDZK1^{PDZD1*}, pCMVTag2C:PDZK1^{PDZD2*}, pCMVTag2C:PDZK1^{PDZD3*}, and pCMVTag2C:PDZK1^{PDZD4*}, where the respective hydrophobic binding pocket ("*GLGF*") sequence for each PDZ domain (Doyle *et al.*, 1996) was mutated from N^{19}YGF^{22} to *K*^{19}Y*RS*^{22} (Domain 1), S^{144}YGF^{147} to S^{144}Y*RE*^{147} (Domain 2), G^{252}YGF^{255} to G^{252}Y*RE*^{255} (Domain 3), and G^{387}YGF^{390} to G^{387}Y*RE*^{390} (Domain 4), were generated by QuikChange site-directed mutagenesis using pCMVTag2C:PDZK1 as template and the primer pairs shown in Supplemental Table 1. Mutations were designed to disrupt PDZ ligand-binding at each domain solely through destabilization of the hydrophobic binding pocket of each PDZ domain, and were validated through the use of the online protein domain organization tool, Pfam (Finn *et al.*, 2010). Conversion of Ser^{505} to Ala^{505} or Asp^{505} to generate pCMVTag2C:PDZK1^{S505A} and pCMVTag2C:PDZK1^{S505D} was also achieved by QuikChange site-directed mutagenesis using pCMVTag2C:PDZK1 as a template and the primer pairs shown in Supplemental Table 1. All mutations were validated by DNA sequence analysis.

Y2H screening and yeast matings

Y2H screening of a human kidney cDNA library with the carboxyl-terminal (C-tail) domain, encoding amino acids 299–386, of the hIP (hIP$^{299–386}$) as specific bait was carried out as previously described (Wikstrom *et al.*, 2008; Reid *et al.*, 2010). Y2H screening identified several independent clones encoding amino acids 1–154 of PDZK1, expressed in the yeast prey plasmid pACT2:PDZK1, as an interactant of the hIP. pGBKT7 and pGBKT7:p53, encoding the GAL4 DBD alone or as a fusion with p53, were obtained from Clontech. All yeast protocols were standard procedures as previously described (Wikstrom *et al.*, 2008). For analysis of protein expression in *Saccharomyces cerevisiae* (*S.c*). AH109 (pGBKT7) bait transformants, protein was extracted, resolved by SDS–PAGE, and screened by Western blot analysis using anti-Myc (9B11), with chemiluminescence detection.

Cell culture and transfections

Human embryonic kidney (HEK) 293 cells were obtained from the American Type Culture Collection (Manassas, VA) and grown in minimal essential medium (MEM) containing 10% fetal bovine serum (FBS). HEK 293 cells were transiently or stably transfected using the calcium phosphate/DNA coprecipitation or Effectene procedures, as previously described (O'Keeffe *et al.*, 2008; Wikstrom *et al.*, 2008). In brief, ~48 h prior to transfection, cells were routinely plated at a density of 2×10^6 cells per 10-cm culture dish in 8 ml media. Thereafter, cells were transiently cotransfected with pcDNA/pCMV-based vector in the presence of pADVA (Gorman *et al.*, 1990) at a ratio of 2.5:1 using either the calcium phosphate/DNA coprecipitation procedure, where a total of 35 μg DNA was used, or the Effectene (Qiagen, Valencia, CA) transfection procedure, where a total of 2 μg DNA was used. HEK.hIP, HEK.hIP^{SSLC}, HEK.hIP$^{\Delta383}$ cells stably overexpressing HA-tagged forms of the wild-type and mutated hIPs, respectively, have been described (Miggin *et al.*, 2003). Primary (1°) human umbilical vein endothelial cells (HUVECs), obtained from Lonza (IRT9-048-0904D; Basel, Switzerland), were routinely cultured in M199 media (Sigma-Aldrich) supplemented with 0.4% (vol/vol) Endothelial Cell Growth Supplement/Heparin (ECGS/H; Lonza), 20% (vol/vol) FBS, and 0.2% (vol/vol) L-glutamine. 1° HUVECs were used between passages 2 and 8. All mammalian cells were grown at 37°C in a humid environment with 5% CO_2 and confirmed to be mycoplasma free.

Immunoprecipitations

HEK.hIP, HEK.hIP^{SSLC}, HEK.hIP$^{\Delta383}$, and HEK.TPα cells were transiently cotransfected with pADVA and either pCMVTag2C:PDZK1 or mutant variants where specified, using Effectene. To assess the effect of the farnesyl transferase inhibitors (FTIs), R115777 and SCH66336, on the interaction between the hIP and PDZK1, HEK.hIP^{WT} cells, transiently cotransfected with pCMVTag2C:PDZK1 were incubated 24 h posttransfection with R115777 and SCH66336 at concentrations indicated in the figure legends, or, as a control, with 0.1% dimethyl sulfoxide (DMSO) (vehicle), for 24 h at 37°C prior to immunoprecipitation. IP-mediated phosphorylation of PDZK1 was examined in HEK.hIP^{WT} cells, transiently cotransfected with pCMVTag2C:PDZK1, whereby cells were preincubated with RO1138452 (10 μM; 10 min) prior to cicaprost stimulation. To assess the effect of the kinase inhibition, H-89, KT5720 and GÖ6983, on the interaction between the hIP and PDZK1, HEK.hIP^{WT} cells, transiently cotransfected with pCMVTag2C:PDZK1 or mutated variants were incubated 48 h posttransfection with H-89, KT5720, and GÖ6983 at concentrations indicated in the figure legends, or, as control, with 0.1% DMSO (vehicle), for 10 min at 37°C prior to immunoprecipitation or stimulation with cicaprost, as indicated. Primary HUVECs were plated onto 10-cm dishes to achieve >80% confluence. In all cases, prior to immunoprecipitation, cells were washed in the appropriate serum-free media and incubated with either vehicle or 1 μM cicaprost for the times indicated in the figure legends. Thereafter, cells were washed, lysed, and clarified as per previously detailed protocols (Wikstrom *et al.*, 2008; Reid *et al.*, 2010). HA-tagged hIP or TPα were immunoprecipitated using anti-HA (101R; 1:300) antibody, FLAG-tagged PDZK1 was immunoprecipitated with anti-FLAG M2 (1:200), endogenously expressed hIP with the affinity purified rabbit polyclonal anti-hIP (1:50) antibody (Reid *et al.*, 2010) or as control, with normal rabbit IgG (Santa Cruz). Thereafter,

lysates were incubated for 1 h with either 50% slurry of protein G-sepharose (10 µl) or protein A-sepharose (immunoprecipitation with rabbit anti-hIP; 40 µl), prior to repeated washing with RIP followed by phosphate-buffered saline (PBS) (two to three times). Immunoprecipitates were resolved by SDS–PAGE and subjected to successive immunoblotting with anti-Flag (1:2500), anti-HA (3F10; 1:500), anti-PDZK1 (1:1000), anti-HDJ-2 (1:4000), and anti-Phospho-Ser (1:1000) antibodies, as indicated.

Immunofluorescence microscopy

To examine the localization of PDZK1 and the hIP, HEK.hIP cells transiently cotransfected with pCMVTag2C:PDZK1 plus pADVA were grown on poly-L-lysine-treated coverslips, in six-well plates for at least 48 h posttransfection. Thereafter, cells were fixed using 3.7% paraformaldehyde in PBS pH 7.4 for 15 min at RT prior to washing in PBS. Cells were permeabilized by incubation with 0.2% Triton X-100 in PBS for 10 min on ice, followed by washing in Tris-buffered saline (TBS). Nonspecific sites were blocked by incubating cells with 1% bovine serum albumin (BSA) in TBS, pH 7.4, for 1 h at RT. Cells were incubated with the affinity purified rabbit polyclonal anti-hIP antibody (1:250; 1% BSA in TBS) to label the hIP and anti-PDZK1 (1:500; 1% BSA in TBS) to label PDZK1 for 1 h at RT. The antibody solution was removed and cells were washed with TBS followed by a further incubation with 1% BSA in TBS-T for 30 min. Cells were then incubated with AlexaFluor488 goat anti–rabbit IgG secondary antibody (1:2000; 1% BSA in TBS-T) to detect the IP receptor and AlexaFluor594 goat anti–mouse IgG secondary antibody (1:4000; 1% BSA in TBS-T) to detect PDZK1 for 1 h at RT. After washing, all slides were counterstained with DAPI (1 µg/ml in H_2O) prior to mounting coverslips in DakoCytomation fluorescence mounting medium. Imaging was carried out using the Zeiss Axioplan 2 microscope and Axioplan Version 4.4 imaging software. Data presented are representative images for at least three independent experiments from which at least 10 fields were viewed at 63× magnification, where the horizontal bar represents 10 µM.

Radioligand binding assays

To examine the effect PDZK1 on hIP expression, HEK.hIP cells were transiently cotransfected with pADVA in the presence of pCMVTag2C:PDZK1 or, as controls, with pCMVTag2C. RLBAs of the hIP were carried out as previously described (Hayes *et al.*, 1999). For saturation binding studies, RLBAs were carried out on cell membranes in the presence of 4 nM [^{3}H]iloprost (15.3 Ci/mmol) at 30°C for 1 h using 50–100 µg of protein in 100 µl reactions. Nonspecific binding was determined in the presence of 0.2 mM iloprost for saturation-binding studies. Alternatively to analyze cell surface hIP expression, following harvesting and washing in PBS, cells were resuspended in MES/KOH buffer and RLBAs were carried out at 4°C for 1 h using whole cell protein in 100-µl reactions. Incubations were terminated by the addition of 4 ml of ice-cold resuspension buffer followed by filtration through Whatman GF/C filters, which had been pretreated in 0.33% polyethyleneimine (PEI) for 1–24 h. The filters were washed three times with resuspension buffer (4 ml) and then subjected to liquid scintillation counting in scintillation fluid (5 ml/filter) using a Tri-Carb 2900TR Liquid Scintillation Analyzer (Perkin Elmer).

Flow cytometry

HEK.hIP cells were transiently cotransfected with pCMVTag2C:PDZK1 or, as a control, with pCMVTag2C along with pADVA using Effectene. Seventy-two hours posttransfection, cells were washed twice with PBS, harvested, and resuspended at 10^6 cells/ml in ice-cold PBS/2% BSA. Cell suspensions were incubated with 2.5 µg/ml anti-HA (101R) antibody or, as a control, with 2.5 µg/ml normal mouse IgG to quantify background fluorescence. After 1 h on ice, the cells were centrifuged at 500 × *g* for 5 min and washed twice in ice-cold PBS/2% BSA. Cell suspensions were then incubated with 1.5 µg/ml AlexaFluor488 goat anti-mouse antibody for 1 h on ice, centrifuged, washed twice in ice-cold PBS/2% BSA and fixed with 3.7% paraformaldehyde in PBS. Surface fluorescence was analyzed on a CyAn ADP using Summit 4.3 software (Dako, Carpinteria, CA). The isotype-matched normal mouse IgG antibody was used to set the gates for positive staining and positively stained cells were gated by forward- and side-scatter. Fluorescent intensity was corrected for background fluorescence, and results are presented as mean fold increase in fluorescent intensity upon PDZK1 overexpression where levels upon control transfection are expressed as 1.

Measurement of agonist-induced cAMP generation

A gene reporter-based assay was performed to investigate the effect of overexpression of PDZK1 on changes in intracellular cAMP levels in response to stimulation of the hIP with its selective agonist cicaprost, essentially as previously described (Turner and Kinsella, 2010). In brief, the plasmids pHM6:hIP (1.5 µg), pCMVTag2C:PDZK1 (2 µg), pCMVTag2C:PDZK^{PDZD1*} (2 µg), pCMVTag2C:PDZK^{PDZD2*} (2 µg), pCMVTag2C:PDZK^{PDZD3*} (2 µg), pCMVTag2C:PDZK^{PDZD4*} (2 µg) or, as a negative control, pCMVTag2C, were each transiently cotransfected into HEK 293 cells with the luciferase reporter pCRE-Luc (1 µg), pRL-TK (50 ng), and pADVA (0.5 µg) using Effectene reagent as per the manufacturer's instructions (Qiagen). Cells were treated 72 h posttransfection with 3-isobutyl-1-methylxanthine (IBMX; 100 µM) at 37°C for 30 min and then stimulated with either vehicle (V; 0.01% DMSO) or 1 µM cicaprost at 37°C for 3 h. Firefly and renilla luciferase activity was assayed 76 h posttransfection using the Dual Luciferase Assay System. Relative firefly to renilla luciferase activities (arbitrary units) were calculated as a ratio and were expressed in relative luciferase units (RLU).

Disruption of PDZK1 expression by siRNA

For siRNA experiments, 1° HUVEC cells were plated at ~2.5 × 10^5 cells/35-mm plate and some 24 h prior to transfection such that cells reach ~50% confluence. Thereafter, cells were transfected with 30 nM PDZK1 siRNA (siRNA$_{PDKZ1}$; 5′-GAAGAACAAUGAUCUGGUAtt; nucleotides 828–846; Dharmacon, Lafayette, CO), 30 nM Lamin A/C siRNA (siRNA$_{LaminA/C}$; 5′-CUGGACUUCCAGAAGAACAtt; Qiagen), or 30 nM scrambled negative control siRNA (siRNA$_{CONTROL}$; 5′-AATTCTCCGAACGTGTCACGTtt-3′; Qiagen) using RNAiFECT transfection reagent (Qiagen), as per manufacturer's instructions. To confirm the efficacy of the siRNA to disrupt PDZK1 expression, following transfection 1° HUVECs were harvested after incubation at 0–72 h and subject to SDS–PAGE (10–15 µg/lane on 10% polyacrylamide gels) followed by electroblotting onto PDVF membranes (Roche). Membranes were successively screened using anti-PDZK1 and anti–Lamin A/C antibodies and then screened using anti-HDJ-2 antibody to confirm uniform protein loading. For migration and tube formation assays, 24 h post siRNA transfection, cells were placed in reduced serum growth media (2.5% FBS) for 16 h before experiments were performed.

Cell migration assays

To monitor changes in 1° HUVEC migration, cells were plated in 12-well plates such that they were ≥90% confluent 24 h postseeding. Thereafter, cells were preincubated in reduced serum media (2.5% FBS) 12–16 h prior to scoring the cells from top-to-bottom perpendicular to predrawn lines (two parallel lines ~3–4 mm) on the

underside of the well using a 200-µl pipette tip. Loose cells and debris were washed away with serum-free media and replaced with reduced serum media (2.5% FBS). Cells were preincubated with vehicle (0.01% PBS) or 10 µM RO1138452 for 10 min prior to stimulation with vehicle (0.01% PBS), cicaprost (1 µM), VEGF (50 ng/ml), or HDL (50 µg/ml), alone or in combination. Immediately (0 h) and after 12-h incubations, the reduction in scratch paths were visualized and imaged using a Nikon TMS inverted microscope with Matrox Intellicam software (Version 2.07) and analyzed with TScratch software (Version 1.0). Migration was expressed as percentage of basal cell migration. All experiments were performed in triplicate, and each experiment was repeated at least three times.

In vitro tube formation assays

Matrigel tube formation assays were performed to assess in vitro angiogenesis. Growth factor-reduced Matrigel (BD Biosciences, San Jose, CA) was placed in 96-well tissue culture plates (50 µl/well) and allowed to gel at 37°C for at least 30 min. Then 1° HUVECs (4×10^3 cells/well) were seeded in 100 µl reduced serum media (2.5% FBS) and preincubated with vehicle (0.01% PBS) or 10 µM RO1138452 for 10 min prior to stimulation with vehicle (0.01% PBS), cicaprost (1 µM), VEGF (50 ng/ml), or HDL (50 µg/ml), alone or in combination. After 12 h incubation, cell morphology was visualized and imaged using a Nikon TMS inverted microscope with Matrox Intellicam software (Version 2.07; 4 times at random per field). The length of tube was measured at 40× magnification with WCIF ImageJ software (Version 1.37c) and expressed as percentage of basal tube length. All experiments were performed at least in triplicate, and each experiment was repeated at least two times.

Data analyses

Statistical analyses of differences were carried out using one-way or two-way ANOVA followed by post hoc Dunnett's multiple comparison *t* tests, as indicated, throughout employing GraphPad Prism, version 4.00 package. P values of ≤0.05 were considered to indicate a statistically significant difference. As relevant, single, double, and triple symbols signify $p \leq 0.05$, ≤ 0.01, and ≤ 0.001, respectively, for post hoc Dunnett's multiple comparison *t* test analyses.

ACKNOWLEDGMENTS

This work was supported by the Science Foundation of Ireland (Grant SFI:05/IN.1/B19). We are grateful to Maria Hill and Karol English for carrying out the initial Y2H screen.

REFERENCES

Arehart E *et al.* (2008). Acceleration of cardiovascular disease by a dysfunctional prostacyclin receptor mutation: potential implications for cyclooxygenase-2 inhibition. Circ Res 102, 986–993.

Biscetti F *et al.* (2008). Selective activation of peroxisome proliferator-activated receptor (PPAR)alpha and PPAR gamma induces neoangiogenesis through a vascular endothelial growth factor-dependent mechanism. Diabetes 57, 1394–1404.

Biscetti F *et al.* (2009). Peroxisome proliferator-activated receptor alpha is crucial for iloprost-induced in vivo angiogenesis and vascular endothelial growth factor upregulation. J Vasc Res 46, 103–108.

Biscetti F, Pola R (2008). Endothelial progenitor cells and angiogenesis join the PPARty. Circ Res 103, 7–9.

Clark RD, Jahangir A, Severance D, Salazar R, Chang T, Chang D, Jett MF, Smith S, Bley K (2004). Discovery and SAR development of 2-(phenylamino) imidazolines as prostacyclin receptor antagonists [corrected]. Bioorg Med Chem Lett 14, 1053–1056.

Davies SP, Reddy H, Caivano M, Cohen P (2000). Specificity and mechanism of action of some commonly used protein kinase inhibitors. Biochem J 351, 95–105.

Doyle DA, Lee A, Lewis J, Kim E, Sheng M, MacKinnon R (1996). Crystal structures of a complexed and peptide-free membrane protein-binding domain: molecular basis of peptide recognition by PDZ. Cell 85, 1067–1076.

Fenske SA, Yesilaltay A, Pal R, Daniels K, Barker C, Quinones V, Rigotti A, Krieger M, Kocher O (2009). Normal hepatic cell surface localization of the high density lipoprotein receptor, scavenger receptor class B, type I, depends on all four PDZ dmains of PDZK1. J Biol Chem 284, 5797–5806.

Fenske SA, Yesilaltay A, Pal R, Daniels K, Rigotti A, Krieger M, Kocher O (2008). Overexpression of the PDZ1 domain of PDZK1 blocks the activity of hepatic scavenger receptor, class B, type I by altering its abundance and cellular localization. J Biol Chem 283, 22097–22104.

Finn RD *et al.* (2010). The Pfam protein families database. Nucleic Acids Res 38, D211–D222.

Fitzgerald GA (2004). Coxibs and cardiovascular disease. N Engl J Med 351, 1709–1711.

Gorman CM, Gies D, McCray G (1990). Transient production of proteins using an adenovirus transformed cell line. DNA Protein Eng Tech 2, 3–10.

Gryglewski RJ (2008). Prostacyclin among prostanoids. Pharmacol Rep 60, 3–11.

Hayes JS, Lawler OA, Walsh MT, Kinsella BT (1999). The prostacyclin receptor is isoprenylated. Isoprenylation is required for efficient receptor-effector coupling. J Biol Chem 274, 23707–23718.

He T, Lu T, d'Uscio LV, Lam CF, Lee HC, Katusic ZS (2008). Angiogenic function of prostacyclin biosynthesis in human endothelial progenitor cells. Circ Res 103, 80–88.

Hu S, Song E, Tian R, Ma S, Yang T, Mu Y, Li Y, Shao C, Gao S, Gao Y (2009). Systematic analysis of a simple adaptor protein PDZK1: ligand identification, interaction and functional prediction of complex. Cell Physiol Biochem 24, 231–242.

Jemth P, Gianni S (2007). PDZ domains: folding and binding. Biochemistry 46, 8701–8708.

Kato Y, Sai Y, Yoshida K, Watanabe C, Hirata T, Tsuji A (2005). PDZK1 directly regulates the function of organic cation/carnitine transporter OCTN2. Mol Pharmacol 67, 734–743.

Kawabe J, Ushikubi F, Hasebe N (2010a). Prostacyclin in vascular diseases. Recent insights and future perspectives. Circ J 74, 836–843.

Kawabe J *et al.* (2010b). Prostaglandin I2 promotes recruitment of endothelial progenitor cells and limits vascular remodeling. Arterioscler Thromb Vasc Biol 30, 464–470.

Kocher O, Comella N, Tognazzi K, Brown LF (1998). Identification and partial characterization of PDZK1: a novel protein containing PDZ interaction domains. Lab Invest 78, 117–125.

Kocher O, Krieger M (2009). Role of the adaptor protein PDZK1 in controlling the HDL receptor SR-BI. Curr Opin Lipidol 20, 236–241.

Kocher O, Yesilaltay A, Cirovic C, Pal R, Rigotti A, Krieger M (2003). Targeted disruption of the PDZK1 gene in mice causes tissue-specific depletion of the high density lipoprotein receptor scavenger receptor class B type I and altered lipoprotein metabolism. J Biol Chem 278, 52820–52825.

LaLonde DP, Bretscher A (2009). The scaffold protein PDZK1 undergoes a head-to-tail intramolecular association that negatively regulates its interaction with EBP50. Biochemistry 48, 2261–2271.

Lamprecht G, Seidler U (2006). The emerging role of PDZ adapter proteins for regulation of intestinal ion transport. Am J Physiol Gastrointest Liver Physiol 291, G766–G777.

Lawler OA, Miggin SM, Kinsella BT (2001a). The effects of the statins lovastatin and cerivastatin on signaling by the prostanoid IP-receptor. Br J Pharmacol 132, 1639–1649.

Lawler OA, Miggin SM, Kinsella BT (2001b). Protein kinase A-mediated phosphorylation of serine 357 of the mouse prostacyclin receptor regulates its coupling to G(s)-, to G(i)-, and to G(q)-coupled effector signaling. J Biol Chem 276, 33596–33607.

Lee HJ, Zheng JJ (2010). PDZ domains and their binding partners: structure, specificity, and modification. Cell Commun Signal 8, 8.

Li Z, Benard O, Margolskee RF (2006). Ggamma13 interacts with PDZ domain-containing proteins. J Biol Chem 281, 11066–11073.

Miggin SM, Lawler OA, Kinsella BT (2002). Investigation of a functional requirement for isoprenylation by the human prostacyclin receptor. Eur J Biochem 269, 1714–1725.

Miggin SM, Lawler OA, Kinsella BT (2003). Palmitoylation of the human prostacyclin receptorFunctional implications of palmitoylation and isoprenylation. J Biol Chem 278, 6947–6958.

Murata T *et al.* (1997). Altered pain perception and inflammatory response in mice lacking prostacyclin receptor. Nature 388, 678–682.

Nakamura T, Shibata N, Nishimoto-Shibata T, Feng D, Ikemoto M, Motojima K, Iso ON, Tsukamoto K, Tsujimoto M, Arai H (2005). Regulation of SR-BI

protein levels by phosphorylation of its associated protein, PDZK1. Proc Natl Acad Sci USA 102, 13404–13409.
Navarro-Lerida I, Martinez-Moreno M, Ventoso I, Alvarez-Barrientos A, Rodriguez-Crespo I (2007). Binding of CAP70 to inducible nitric oxide synthase and implications for the vectorial release of nitric oxide in polarized cells. Mol Biol Cell 18, 2768–2777.
O'Keeffe MB, Reid HM, Kinsella BT (2008). Agonist-dependent internalization and trafficking of the human prostacyclin receptor: a direct role for Rab5a GTPase. Biochim Biophys Acta 1783, 1914–1928.
O'Meara SJ, Kinsella BT (2004a). Effect of the statin atorvastatin on intracellular signaling by the prostacyclin receptor in vitro and in vivo. Br J Pharmacol 143, 292–302.
O'Meara SJ, Kinsella BT (2004b). Investigation of the effect of the farnesyl protein transferase inhibitor R115777 on isoprenylation and intracellular signaling by the prostacyclin receptor. Br J Pharmacol 143, 318–330.
O'Meara SJ, Kinsella BT (2005). The effect of the farnesyl protein transferase inhibitor SCH66336 on isoprenylation and signaling by the prostacyclin receptor. Biochem J 386, 177–189.
Patrignani P *et al*. (2008). Differential association between human prostacyclin receptor polymorphisms and the development of venous thrombosis and intimal hyperplasia: a clinical biomarker study. Pharmacogenet Genomics 18, 611–620.
Pola R, Gaetani E, Flex A, Aprahamian TR, Bosch-Marce M, Losordo DW, Smith RC, Pola P (2004). Comparative analysis of the in vivo angiogenic properties of stable prostacyclin analogs: a possible role for peroxisome proliferator-activated receptors. J Mol Cell Cardiol 36, 363–370.
Qu Y, Shi X, Zhang H, Sun W, Han S, Yu C, Li J (2009). VCAM-1 siRNA reduces neointimal formation after surgical mechanical injury of the rat carotid artery. J Vasc Surg 50, 1452–1458.
Reid HM, Mulvaney EP, Turner EC, Kinsella BT (2010). Interaction of the human prostacyclin receptor with Rab11: characterization of a novel Rab11 binding domain within alpha-helix 8 that is regulated by palmitoylation. J Biol Chem 285, 18709–18726.
Reid HM, Wikstrom K, Kavanagh DJ, Mulvaney EP, Kinsella BT (2011). Interaction of angio-associated migratory cell protein with the TPalpha and TPbeta isoforms of the human thromboxane A(2) receptor. Cell Signal 23, 700–717.
Ribeiro LG, Brandon TA, Hopkins DG, Reduto LA, Taylor AA, Miller RR (1981). Prostacyclin in experimental myocardial ischemia: effects on hemodynamics, regional myocardial blood flow, infarct size and mortality. Am J Cardiol 47, 835–840.
Tonikian R *et al*. (2008). A specificity map for the PDZ domain family. PLoS Biol 6, e239.
Turner EC, Kinsella BT (2010). Estrogen increases expression of the human prostacyclin receptor within the vasculature through an ERalpha-dependent mechanism. J Mol Biol 396, 473–486.
Voltz JW, Brush M, Sikes S, Steplock D, Weinman EJ, Shenolikar S (2007). Phosphorylation of PDZ1 domain attenuates NHERF-1 binding to cellular targets. J Biol Chem 282, 33879–33887.
Wang S, Yue H, Derin RB, Guggino WB, Li M (2000). Accessory protein facilitated CFTR-CFTR interaction, a molecular mechanism to potentiate the chloride channel activity. Cell 103, 169–179.
Wikstrom K, Reid HM, Hill M, English KA, O'Keeffe MB, Kimbembe CC, Kinsella BT (2008). Recycling of the human prostacyclin receptor is regulated through a direct interaction with Rab11a GTPase. Cell Signal 20, 2332–2346.
Yuhki K, Kojima F, Kashiwagi H, Kawabe J, Fujino T, Narumiya S, Ushikubi F (2011). Roles of prostanoids in the pathogenesis of cardiovascular diseases: novel insights from knockout mouse studies. Pharmacol Ther 129, 195–205.
Zhu W, Saddar S, Seetharam D, Chambliss KL, Longoria C, Silver DL, Yuhanna IS, Shaul PW, Mineo C (2008). The scavenger receptor class B type I adaptor protein PDZK1 maintains endothelial monolayer integrity. Circ Res 102, 480–487.